(u)

SECURITY CLASSIFICATION OF THIS PAGE

DTIC FILE COPY

(2)

REPORT DOCUMENTATION PAGE

AD-A222 549

DTIC ELECTE MAY 29 1990 S D D

	1b. RESTRICTIVE MARKINGS
	3. DISTRIBUTION/AVAILABILITY OF REPORT: Unlimited. Approved for public release, distribution unlimited
4. PERFORMING ORGANIZATION REPORT NUMBER(S): CMTC-8945	5. MONITORING ORGANIZATION REPORT NUMBER(S): AFOSR-TR- 90-0569
6a. NAME OF PERFORMING ORGANIZATION: Penn State University; 6b. OFFICE SYMBOL (If applicable):	7a. NAME OF MONITORING ORGANIZATION: AFOSR
6c. ADDRESS (City, State and ZIP Code): 227 Hammond Building, University Park, PA 16802	7b. ADDRESS (City, State and ZIP Code): AFOSR/NA Bldg 410, Bolling AFB DC 20332-6448
8a. NAME OF FUNDING/SPONSORING ORGANIZATION: Air Force Office of Scientific Research; 8b. OFFICE SYMBOL (If applicable): NA	9. PROCUREMENT INSTRUMENT IDENTIFICATION NUMBER: Grant: AFOSR-87-0242
8c. ADDRESS (City, State and ZIP Code): Bolling Air Force Base, Washington, DC 20332-6448	10. SOURCE OF FUNDING NOS.: PROGRAM ELEMENT NO. 61102F; PROJECT NO. 2302; TASK NO. B2; WORK UNIT NO.

11. TITLE (Include Security Classification): Prediction and Control of Processing-Induced Residual Stresses in Composites Part I: IM6/BMI Composite (Unclassified)

12. PERSONAL AUTHOR(S): White, Scott R., Hahn, Hong T.

13a. TYPE OF REPORT	13b. TIME COVERED	14. DATE OF REPORT (Yr., Mo., Day)	15. PAGE COUNT
Final Report	FROM 6-87 TO 6-89	89-September-1	81

16. SUPPLEMENTARY NOTATION

17. COSATI CODES: FIELD	GROUP	SUB. GR.

18. SUBJECT TERMS (Continue on reverse if necessary and identify by block number): Plastics, Thermoplastic Matrix Composite, PEEK, Mechanical Properties, Crystals, Polymers (JG)

19. ABSTRACT (Continue on reverse if necessary and identify by block number)

Residual stresses are developed during processing of composites due to the thermal mismatch between constituents and the chemical shrinkage of the matrix during the crosslinking reaction. Our research has shown that these residual stresses can be high enough to cause ply cracking even before loading.

The objectives of the present research were to determine how residual stresses develop during processing, develop a model which would predict these residual stresses, and find an optimization scheme which would reduce the residual stresses induced by processing.

The approach taken was to monitor the residual stress development through the curvature measurements in unsymmetric cross-ply specimens. The material system used was a graphite/BMI manufactured by American Cyanamid under the trade name CYCOM 3100™. Both elastic and viscoelastic models were used to predict the induced curvature. Mechanical testing and thermal analysis of processed specimens provided the input data for modeling. Drawing from the experimental results and analytical modeling, several cure cycle variations were proposed and investigated to reduce residual stresses.

20. DISTRIBUTION/AVAILABILITY OF ABSTRACT	21. ABSTRACT SECURITY CLASSIFICATION
UNCLASSIFIED/UNLIMITED X SAME AS RPT. ☐ DTIC USERS ☐	(u)
22a. NAME OF RESPONSIBLE INDIVIDUAL: [redacted] George K. Haritos	22b. TELEPHONE NUMBER: [redacted] (202) 767-0463; 22c. OFFICE SYMBOL: NA

DD FORM 1473, 83 APR EDITION OF 1 JAN 73 IS OBSOLETE.

SECURITY CLASSIFICATION OF THIS PAGE (u)

90 05 29 138

Block 19 Continued...

Our research has shown that the processing-induced residual stress development is elastic. If transverse cracking is developed elastic analysis will overestimate the curvature since transverse cracking relieves the residual stresses in the laminate. The transverse strength develops slower than the transverse modulus during cure and, thus, transverse cracking can occur if the degree of cure is not sufficient to allow transverse strength development. In the BMI system specimens with degrees of cure greater that 0.89 did not show signs of transverse cracking.

Thermal strains are dominant in residual stress development in thermosetting resin systems. Therefore, residual stresses can be reduced by curing at lower temperatures. The mechanical properties and degree of cure are not sacrificed if dwell times are increased as well. Promising results were shown for BMI in which the residual stresses in the form of dimensionless curvature were reduced by 14% by processing at 320 F for 12 hours. The degree of cure in this case was 0.95 indicating a nearly complete reaction.

Future work should include development of the cure kinetics of the resin. Knowledge of the cure kinetics will allow for optimum choice of dwell time and cure temperature to allow complete cure. Assuring complete cure is necessary to retain good mechanical properties after processing.

PENN STATE

CMTC - 8945

PREDICTION AND CONTROL OF PROCESSING-INDUCED RESIDUAL STRESSES IN COMPOSITES

PART I: IM6/BMI COMPOSITE

S.R. WHITE
H.T. HAHN

OCTOBER 1989

Final Technical Report

Prepared for:
Air Force Office of Scientific Research
under AFOSR Grant 87-0242

Composites Manufacturing Technology Center
227 Hammond Building
The Pennsylvania State University
University Park, PA 16802

Table of Contents

List of Figures iii

List of Tables v

Abstract vi

1. Introduction 1

2. Analysis 4

2.1 Elastic Analysis 4

2.2 Viscoelastic Analysis 7

3. Experimental Procedure 10

3.1 Intermittent Cure Technique 10

3.1.1 Curvature Development 10

3.1.2 Mechanical Property Testing 14

3.1.2.1 Longitudinal Properties 14

3.1.2.2 Transverse Properties 16

3.1.3 DSC Testing 16

3.1.4 Thermal Strains 19

3.2 Postcure 19

3.3 Creep Testing 22

3.4 Cure Cycle Optimization 25

4. Results and Discussion 26

4.1 Mechanical Properties 26

4.2 DSC Testing 33

4.3 Thermal Strains 37

4.4 Elastic Analysis 41

4.5 Chemical Shrinkage 46

4.6 Postcure 47

4.7 Viscoelastic Modeling 50

4.8 Cure Cycle Optimization 55

4.8.1 Effect of Cure Temperature 55

4.8.2 Effect of Cool-Down Rate 62

4.8.3 Effect of Cool-Down Pressure 66

5. Summary 70

6. Acknowledgement 72

7. References 73

8. Appendix - Participating Professionals 75

9. Appendix - Publications 76

DTIC COPY INSPECTED 1

Accesion For
NTIS CRA&I ☑
DTIC TAB ☐
Unannounced ☐
Justification

By
Distribution /

Availability Codes

Dist	Avail and / or Special
A-1	

List of Tables

1. Creep Testing Matrix 24

2. Input Parameters for Equation (7) 42

3. Change in Curvature Predicted after Postcure 49

4. Viscoelastic Model Input Data 53

5. Processing Conditions for Cure Cycle Optimization Study 56

Abstract

Residual stresses are developed during processing of composites due to the thermal mismatch between constituents and the chemical shrinkage of the matrix during the crosslinking reaction. Our research has shown that these residual stresses can be high enough to cause ply cracking even before loading.

The objectives of the present research were to determine how residual stresses develop during processing, develop a model which would predict these residual stresses, and find an optimization scheme which would reduce the residual stresses induced by processing.

The approach taken was to monitor the residual stress development through the curvature measurements in unsymmetric cross-ply specimens. The material system used was a graphite/BMI manufactured by American Cyanamid under the trade name CYCOM 3100™. Both elastic and viscoelastic models were used to predict the induced curvature. Mechanical testing and thermal analysis of processed specimens provided the input data for modeling. Drawing from the experimental results and analytical modeling, several cure cycle variations were proposed and investigated to reduce residual stresses.

Our research has shown that the processing-induced residual stress development is elastic. If transverse cracking is developed elastic analysis will overestimate the curvature since transverse cracking relieves the residual stresses in the laminate. The transverse strength develops slower than the transverse modulus during cure and, thus, transverse cracking can occur if the degree of cure is not sufficient to allow transverse strength development. In the BMI system specimens with degrees of cure greater that 0.89 did not show signs of transverse cracking.

Thermal strains are dominant in residual stress development in thermosetting resin systems. Therefore, residual stresses can be reduced by curing at lower temperatures. The mechanical properties and degree of cure are not sacrificed if dwell times are increased as well. Promising results were shown for BMI in which the residual stresses in the form of

dimensionless curvature were reduced by 14% by processing at 320 F for 12 hours. The degree of cure in this case was 0.95 indicating a nearly complete reaction.

Future work should include development of the cure kinetics of the resin. Knowledge of the cure kinetics will allow for optimum choice of dwell time and cure temperature to allow complete cure. Assuring complete cure is necessary to retain good mechanical properties after processing.

1. Introduction

The temperature and chemical changes encountered in processing of composites subject the constituent phases to deformational mismatch. To assure compatible deformation residual stresses are developed within the composite. These residual stresses can be high enough to cause ply cracking even before loading. In other situations the residual stresses may not be high enough immediately after processing to cause microcracking, but during the life of the structure, cracks can develop in plies at loads lower than expected.

In general, the processing temperature for most graphite/epoxy systems is not high enough to cause ply cracking. In elevated-temperature resins such as bismaleimide and various thermoplastics, the processing temperature is higher and this leads to higher residual stresses. At room temperature moisture absorption can be beneficial in reducing residual stresses . However, the elevated-temperature resins show less moisture affinity compared with epoxies.

Residual stresses which induce ply cracking are detrimental to the service life of composite structures. Under long-term service these ply cracks will accelerate moisture diffusion, promote delaminations, expose fibers to harmful environments, and reduce mechanical properties such as fracture toughness, strength, endurance limit, etc.

The earliest analysis of residual stresses in composites was based on the assumption of elastic behavior [1,2]. This type of analysis starts after complete cure and, hence does not take into account the chemical shrinkage. Chemical shrinkage has been investigated separately in [3-5]. These studies are limited to neat resin testing and do not integrate the thermal and mechanical strains found in processed composites.

Viscoelastic analysis of cured laminates can be found in [6-10]. A combined effect of temperature and moisture was addressed in [8,9] whereas optimum cooling paths to

reduce residual stresses were investigated in [10]. Viscoelastic analysis shows lower residual stresses upon cool-down compared with elastic analysis, as is to be expected.

A convenient method of monitoring residual stresses is the use of unsymmetric cross-ply laminates [2,6,11-15]. When a small laminate is used the classical laminated plate theory can be used in the analysis. However, for large laminates which allow large deformations, the resulting geometric nonlinearities should be taken into account [11,15]. For long, narrow strips the classical laminated plate theory has been shown to be valid [14].

Although residual stresses and their effects on structural integrity have been analyzed in the past, the process of residual stress development during cure is not well known. Other researchers have limited their scope to analysis during and after the cool-down phase of cure. Serious attempts at delineating relationships between cure cycle and residual stresses are sparce. Before the present research only two papers could be found in this regard [3,16]. In the former, the residual stress development in a neat resin was found to be negligible until cure is almost complete. In the latter, a longer dwell time at gelation was found to reduce residual stresses in a graphite/epoxy laminate.

The objectives of the present research were to determine how residual stresses develop during processing, develop a model which would predict these residual stresses, and find an optimization scheme which would reduce the residual stresses induced by processing.

The approach taken was to monitor the residual stress development through the curvature measurements in unsymmetric cross-ply specimens. The material system used was a thermosetting graphite/BMI manufactured by American Cyanamid under the trade name CYCOM 3100™. BMI composites have become very popular because of their excellent hot/wet properties. Unfortunately, most BMI's are known to be brittle and suspect to transverse cracking. The higher processing temperature (360°F) of BMI can lead

to higher residual stresses. Higher residual stresses combined with the brittle nature of BMI's can lead to problems with structural integrity in BMI structures.

In the analysis both elastic and viscoelastic models were used to predict the induced curvature. Mechanical testing and thermal analysis of processed specimens provided the input data for modeling. Drawing from the experimental results and analytical modeling, several cure cycle variations were proposed and investigated to reduce residual stresses.

2. Analysis

2.1. Elastic Analysis

The thermoelastic stress-strain relations for orthotropic laminae under plane stress conditions are

$$\sigma_i = Q_{ij}(\varepsilon_j - e_j) \tag{1}$$

where σ is the stress, ε is the strain, and Q is the laminate stiffnesses all at the final temperature T of interest. In (1) e_j is the expansional strain from the stress-free temperature T. During curing, the expansional strain consists of thermal e^T and chemical shrinkage strain e^C,

$$e = e^T + e^C \tag{2}$$

For the crossply $[0_n/90_n]_T$ laminate in Figure 1, the longitudinal and transverse stresses in the individual plies is given by

$$\begin{aligned}
\sigma_{11}^0 &= Q_{11}\varepsilon_1 + Q_{12}\varepsilon_2 - (Q_{11}e_1 + Q_{12}e_2) \\
\sigma_{22}^0 &= Q_{12}\varepsilon_1 + Q_{22}\varepsilon_2 - (Q_{12}e_1 + Q_{22}e_2) \\
\sigma_{11}^{90} &= Q_{22}\varepsilon_1 + Q_{12}\varepsilon_2 - (Q_{22}e_2 + Q_{12}e_1) \\
\sigma_{22}^{90} &= Q_{12}\varepsilon_1 + Q_{11}\varepsilon_2 - (Q_{12}e_2 + Q_{11}e_1)
\end{aligned} \tag{3}$$

In equation (3) the superscripts 0 and 90 refer to the 0° and 90° plies respectively. According to the laminated plate theory, the midplane strains and curvatures at T are calculated by requiring that the stress resultants (N_1, N_2) and the bending moments (M_1, M_2) must be zero.

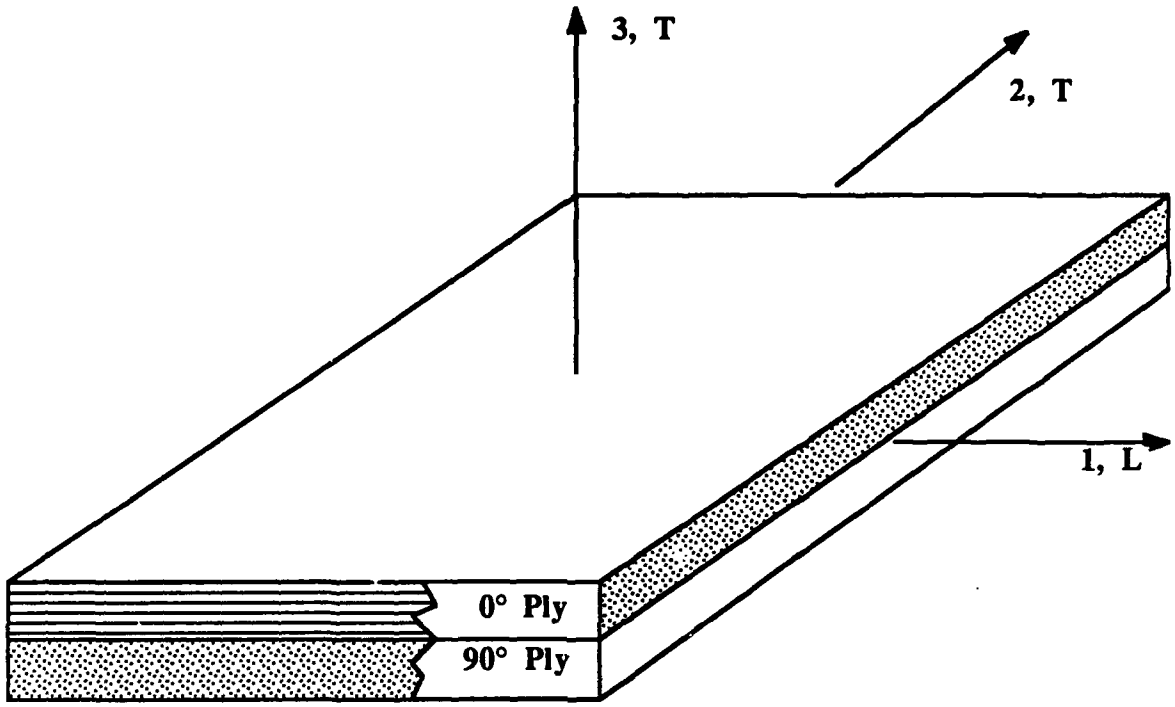

Figure 1. Geometry of an Unsymmetric Cross-ply Plate

$$N_1 = \int_{-h}^{0} \sigma_{11}^{90} dz + \int_{0}^{h} \sigma_{11}^{0} dz = 0$$

$$N_2 = \int_{-h}^{0} \sigma_{22}^{90} dz + \int_{0}^{h} \sigma_{22}^{0} dz = 0$$

$$M_1 = \int_{-h}^{0} \sigma_{11}^{90} \cdot z\, dz + \int_{0}^{h} \sigma_{11}^{0} \cdot z\, dz = 0 \tag{4}$$

$$M_2 = \int_{-h}^{0} \sigma_{22}^{90} \cdot z\, dz + \int_{0}^{h} \sigma_{22}^{0} \cdot z\, dz = 0$$

Substituting equations (3) into (4) and solving for the curvature yields

$$k_a = k_1 = -k_2 = \frac{24}{t} K_a E (e_1 - e_2) \tag{5}$$

where

$$K_a = \frac{(1 - \nu^2 E)}{1 + 14E + (1 - 16\nu^2 E^2} \tag{6}$$

The major Poisson's ration is ν and the ratio of the transverse modulus to the longitudinal modulus (E_T/E_L) is E. Equation (5) gives the induced curvature for anticlastic deformation of an unsymmetric crossply laminate subjected to a temperature change ΔT. The curvature is dependent on the thermal expansion mismatch ($e_1 - e_2$), laminate mechanical properties (ν, E) and the total thickness.

Equation (5) is valid when the overall dimensions of the laminate are small so that the deflections are small. However, for large laminates the deflections may become too large to satisfy the assumptions of linear theory. In this case a large-deflection plate theory must be used [11-13]. For narrow and long strips, the small-deformation laminated plate theory can still be used with the modified condition $k_2 = 0$ in place of $M_2 = 0$. The result is

$$k_c = k_1 = \frac{24}{t} K_c E (e_1 - e_2) \tag{7}$$

where

$$K_c = \frac{\left[1 + (1 - 2\nu - \nu^2)E + (-1 + 2\nu)\nu^2 E^2\right]}{1 + 15E + (15 - 16\nu^2)E^2 + (1 - 16\nu^2)E^3} \tag{8}$$

To account for small thickness variations between different specimens, the dimensionless curvature, $t \cdot k_c$, could be used. Note that $t \cdot k_c$ depends directly on $E(e_1 - e_2)$. Since $E \ll 1$ and $\nu \sim 0.35$ for graphite/BMI composites, the dimensionless curvature is almost proportional to $E(e_1 - e_2)$.

2.2. Viscoelastic Analysis

Polymeric materials are known to exhibit time-dependent mechanical behavior especially at high temperature. This time-dependent behavior may be approximated by a viscoelastic constitutive relationship [7]. For linear thermorheologically simple viscoelastic materials, a single temperature dependent shift factor, $a_T(T)$, can be used to account for the transient thermal response.

The viscoelastic response is history dependent and involves the use of reduced-times, $\xi(t)$ and $\xi(\tau)$. These reduced times are found from the shift factor

$$\xi(t) = \int_0^t \frac{ds}{a_T[T(s)]} \ , \ \xi(\tau) = \int_0^\tau \frac{ds}{a_T[T(s)]} \tag{9}$$

In principle the shift factor will depend on the degree of cure. However, as a first appoximation the shift factor was assumed to be a function of temperature only. For thermorheologically simple behavior the viscoelastic solution can be obtained from the

corresponding elastic solution by means of the correspondence principle. In view of equations (5) and (6) the time-dependent dimensionless curvature is given by [7]

$$t \cdot k_c(t) = \int_0^t F\left[\xi(t) - \xi(\tau)\right] \frac{d}{d\tau}\left(e_1(\tau) - e_2(\tau)\right) d\tau \tag{10}$$

where

$$F(t) = 24\, K_c(t) \tag{11}$$

It is known that the only compliance which exhibits significant time dependent behavior is the transverse compliance, $S_{22}(t)$ [6,7,10,17]. Further, the transverse compliance can be modeled by a power law equation of the form [6,7]

$$S_{22}(t) = S_{22}^0 + D\left(\frac{t}{a_T}\right)^n \tag{12}$$

The parameters D,n, and S_{22}^0 in equation (12) were obtained through experimental correlation to transverse creep experiments. Equation (13) is obtained by substituting laminate compliances for the mechanical properties E and ν in $K_a(t)$ in equation (11).

$$F(t) = \frac{24\left[S_{11}S_{22}(t) - S_{12}^2\right]}{S_{22}^2 + 14S_{11}S_{22}(t) + S_{11}^2 - 16S_{12}^2} \tag{13}$$

The shift factor is an exponential function of temperature:

$$a_T(T) = \exp\left(\frac{-T}{A} + B\right) \tag{14}$$

Equation (10) is solved by discretizing the time domain into n equal portions Δt between the initial time $t_1=0$ and the current time $t_n=t$.

$$t \cdot k_\zeta(t) = \int_0^t F\left[\xi(t) - \xi(\tau)\right] \frac{d\Delta T(\tau)}{d\tau} d\tau = \sum_{k=1}^{n} \int_{t_k}^{t_{k+1}} F\left[\xi(t) - \xi(\tau)\right] \frac{d(e_1 - e_2)}{d\tau} d\tau \qquad (15)$$

$$\approx \frac{1}{2}\sum_{k=1}^{n} \left\{ F\left[\xi(t_{n+1}) - \xi(t_{k+1})\right] + F\left[\xi(t_{n+1}) - \xi(t_k)\right] \right\} \left[\Delta e(t_{k+1}) - \Delta T(t_k)\right] \qquad (16)$$

Solutions to equations (9,12,13,14,16) were computed on a VAX 750 mainframe computer. From equation (16) the dimensionless curvature is seen to be history dependent.

3. Experimental Procedure

3.1. Intermittent Cure Technique

An intermittent cure technique was selected as a means to investigate how residual stresses develop during cure. The manufacturer's recommended cure (MRC) cycle was interrupted at 8 pre-determined points and the specimens cooled down to room temperature at a constant rate of 10°F/min. The specimens obtained were thus incompletely cured and provided information on the development of a number of important properties during the cure cycle. Figure 2 shows the MRC cycle and the intermittent cure points that were selected. All specimens were processed in individual mold cavities on a Tetrahedron MTP-14 Smart Press under computer control. The lay-up sequence used for the specimens is given in Figure 3. Three specimes each of $[0_4/90_4]_T$, $[0]_8$, and $[90]_8$ were cured in the same mold. Once the specimens were manufactured, a series of tests were performed to measure the changes occurring in mechanical properties, residual stresses, and thermal properties.

3.1.1. Curvature Measurement

Thin strips 25.4 mm wide x 152.4 mm long were used to monitor the residual stress development. These strips were $[0_4/90_4]_T$ cross-ply laminates of IM6/BMI composite (American Cyanamid CYCOM 3100™).

These specimens exhibited a cylindrical curvature after processing. This curvature was measured by placing the specimen on a 127 mm base plate and measuring the deflection above the plate. Knowing the deflection (h) and chord length (L) from Figure 4 and measuring the specimen thickness, the dimensionless curvature can be calculated by

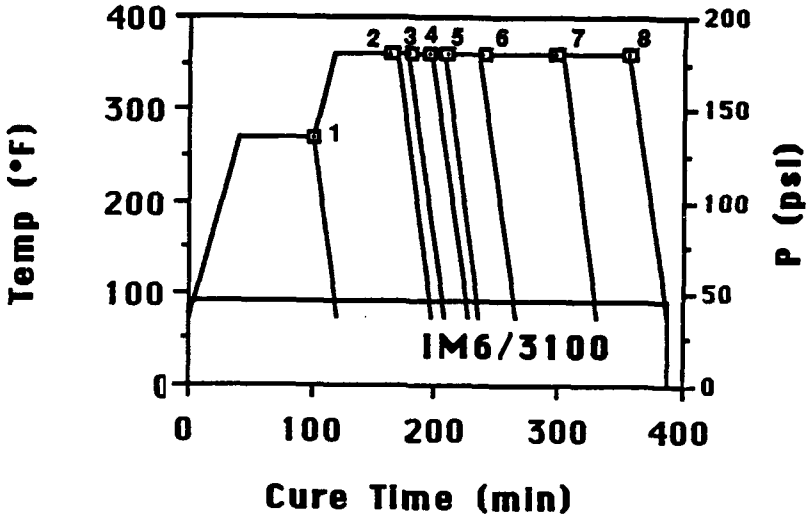

Figure 2. MRC Cycle with 8 Intermittent Cure Points

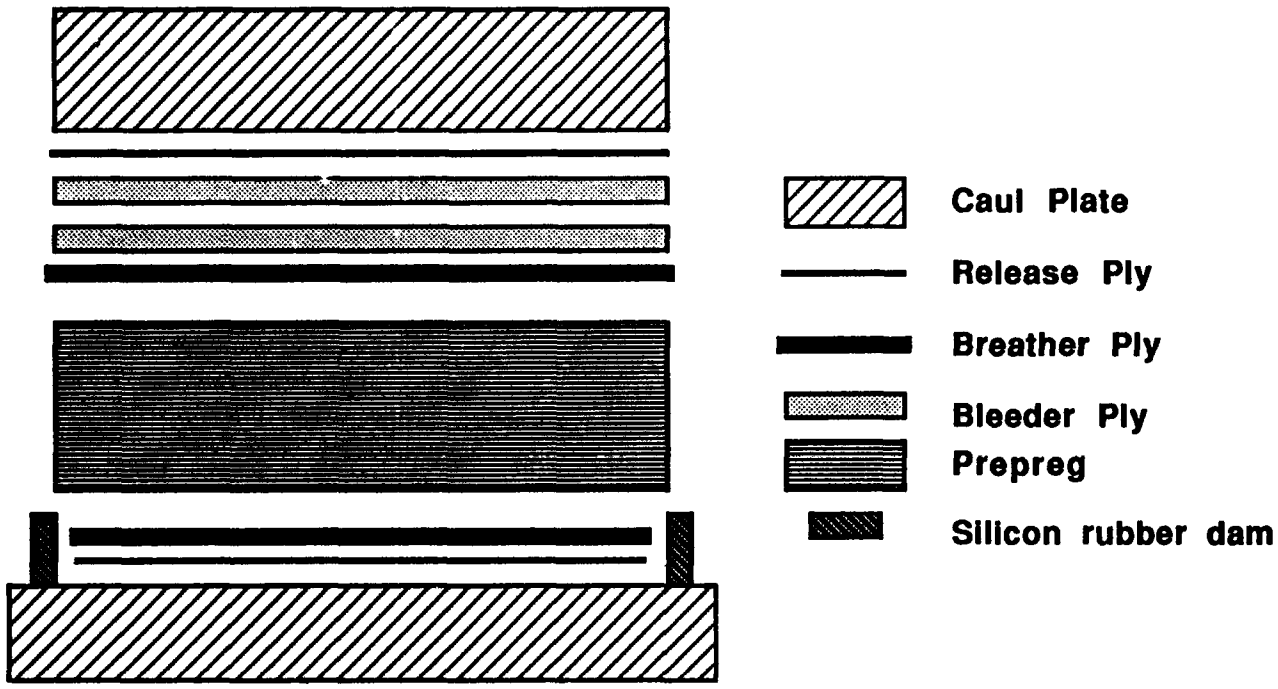

Figure 3. Lay-up Sequence for Hot Press Processing of IM6/3100

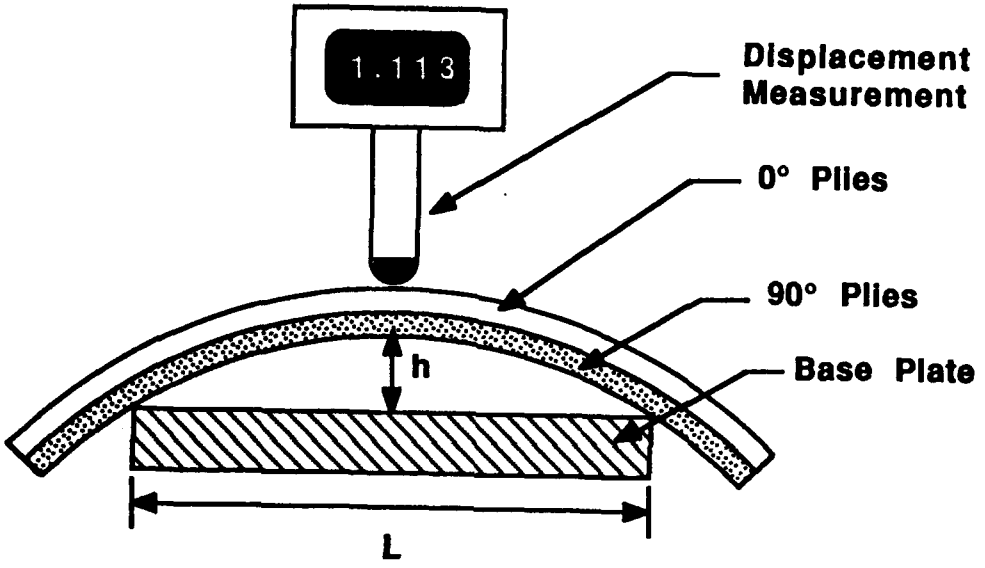

Figure 4. Experimental Curvature Measurement

$$t \cdot k_c = \frac{2 \cdot t \cdot h}{\left(\frac{L^2}{4} + h^2\right)} \tag{17}$$

The dimensionless curvature as measured experimentally by equation (17) is shown in Figure 5 at the various intermittent cure points. The curvature is initially very low but then increases rapidly before approaching the fully cured value of 31.18 x 10e-04. To understand why the residual stresses develop in such a fashion mechanical property tests and DSC analysis were performed on these specimens.

3.1.2. Mechanical Property Testing

3.1.2.1 Longitudinal Properties

The longitudinal mechanical properties of the laminates were characterized by processing $[O]_8$ 12.7 mm x 216 mm specimens with the cross-ply specimens. Three specimens at each of the intermittent cure points were processed and tested. Fiberglass/epoxy end tabs and biaxial strain gages (Micro-Measurements EA-06-125TM-120) were bonded to each specimen. Load and strain data were taken at room temperature in a screwdriven Instron test machine at a crosshead speed of 0.5 mm/min according to ASTM D3039-76. Longitudinal Young's modulus (E_L), longitudinal strength (X_L), and major Poisson's ratio (ν_{LT}) were obtained from the raw test data.

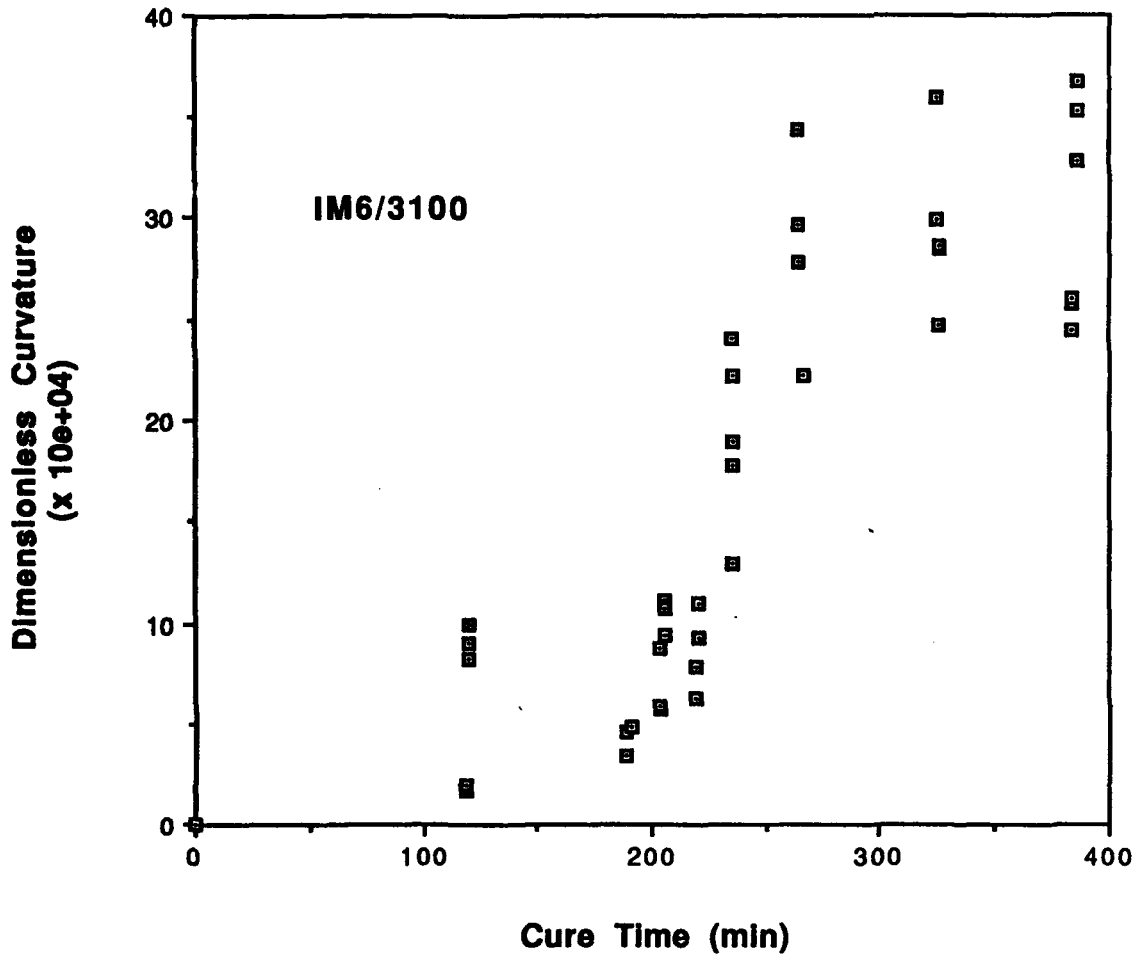

Figure 5. Dimensionless Curvature Development During MRC Cycle (Intermittent Cure Specimens)

3.1.2.2. Transverse Properties

The transverse mechanical properties were obtained by processing $[90]_8$ 12.7 mm x 152.4 mm specimens with the cross ply and longitudinal specimens. At each of the intermittent cure points, five to six transverse specimens were tested. Strain gages (Micro-Measurements EA-06-125AD-120) were bonded to the specimens and tension testing was accomplished in a screwdriven Instron at 0.5 mm/min as was the case in longitudinal testing. The load and strain were monitored at room temperature throughout the testing until final failure.

3.1.3. DSC Testing

To more fully understand the changes in mechanical properties and curvature during the cure cycle a determination of the cure state at each of the intermittent cure points was needed. Differential Scanning Calorimetry (DSC) testing was performed to obtain this information.

A Perkin-Elmer DSC-7 system (Figure 6) was used in the present study with an inert nitrogen atmosphere within the sample cell. Samples of approximately 20 mg of prepreg and intermittently cured specimens were scanned from room temperature to 375°C at 20°C/min. The samples were encapsulated in aluminum sample pans and lids. The differential heat flow between the sample cell and a reference cell (containing an empty aluminum sample pan and lid) was monitored during the dynamic scan. A typical DSC trace of the prepreg is shown in Figure 7. The heat of reaction can be calculated by measuring the area under the curve from the flat baseline. The degree of cure, c , is defined as

$$c = 1 - \frac{H_R}{H_U} \tag{18}$$

Figure 6. Perkin Elmer Series 7 Thermal Analysis System

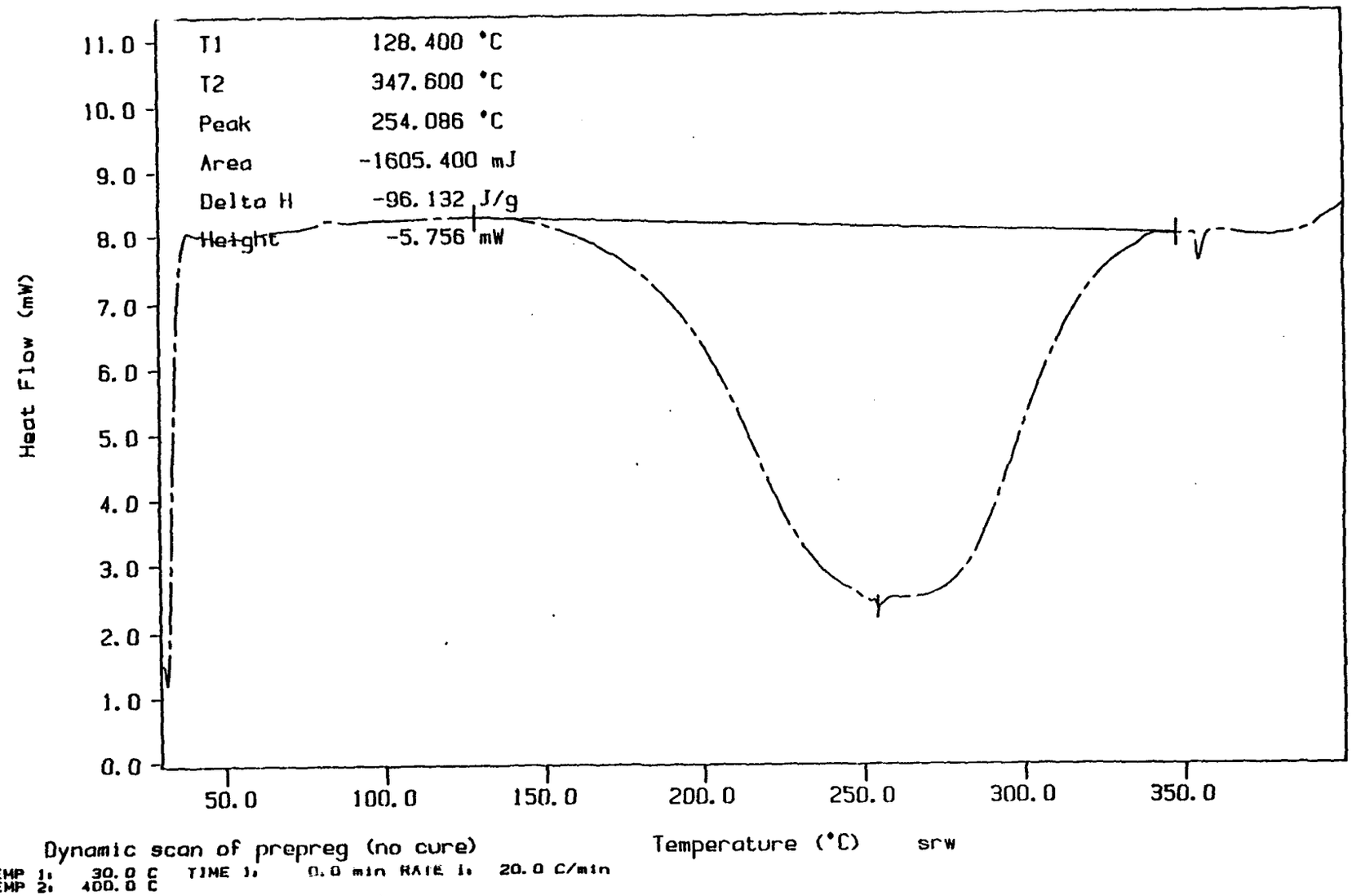

Figure 7. DSC Dynamic Scan of IM6/3100 Prepreg

where H_R is the residual exotherm and H_U is the ultimate heat of reaction. The residual exotherms for the intermittently cured samples were measured from the DSC traces and the ultimate heat of reaction was taken as the area under the exotherm of the prepreg. Thus the degree of cure reported is a relative value since the prepreg is assumed to be uncured ($c = 0$). The ultimate heat of reaction of the prepreg was measured to be 95.8 J/g.

3.1.4. Thermal Strains

Unidirectional $[90]_8$ specimens were processed intermittently to obtain both longitudinal and transverse thermal strains. Strain gages (Micro-Measurement CEA-06-125UN-20) were bonded to the surface of the outermost ply during the lay-up process. Leads were connected and kept electrically insulated through a suitable lay-up sequence (see Figure 8). A type-J thermocouple was mounted to the surface of the specimen to provide a continuous monitor of specimen temperature. Strain and temperature data were collected throughout the cure cycle with an Omega 900 data acquisition system.

3.2. Postcure

Postcure is recommended for thermosetting resin systems in order to assure complete cure and obtain optimum mechanical properties. The postcure cycle recommended for the BMI system investigated is given in Figure 9. The intermittently cured specimens were subjected to this postcure cycle free standing in an oven. The curvature and weight before and after postcure were monitored. During postcure the undercured specimens were expected to become fully cured. As confirmation, DSC traces of postcure samples showed no discernable residual exotherm. The results were analyzed to determine changes in residual stress and mechanical properties after postcure.

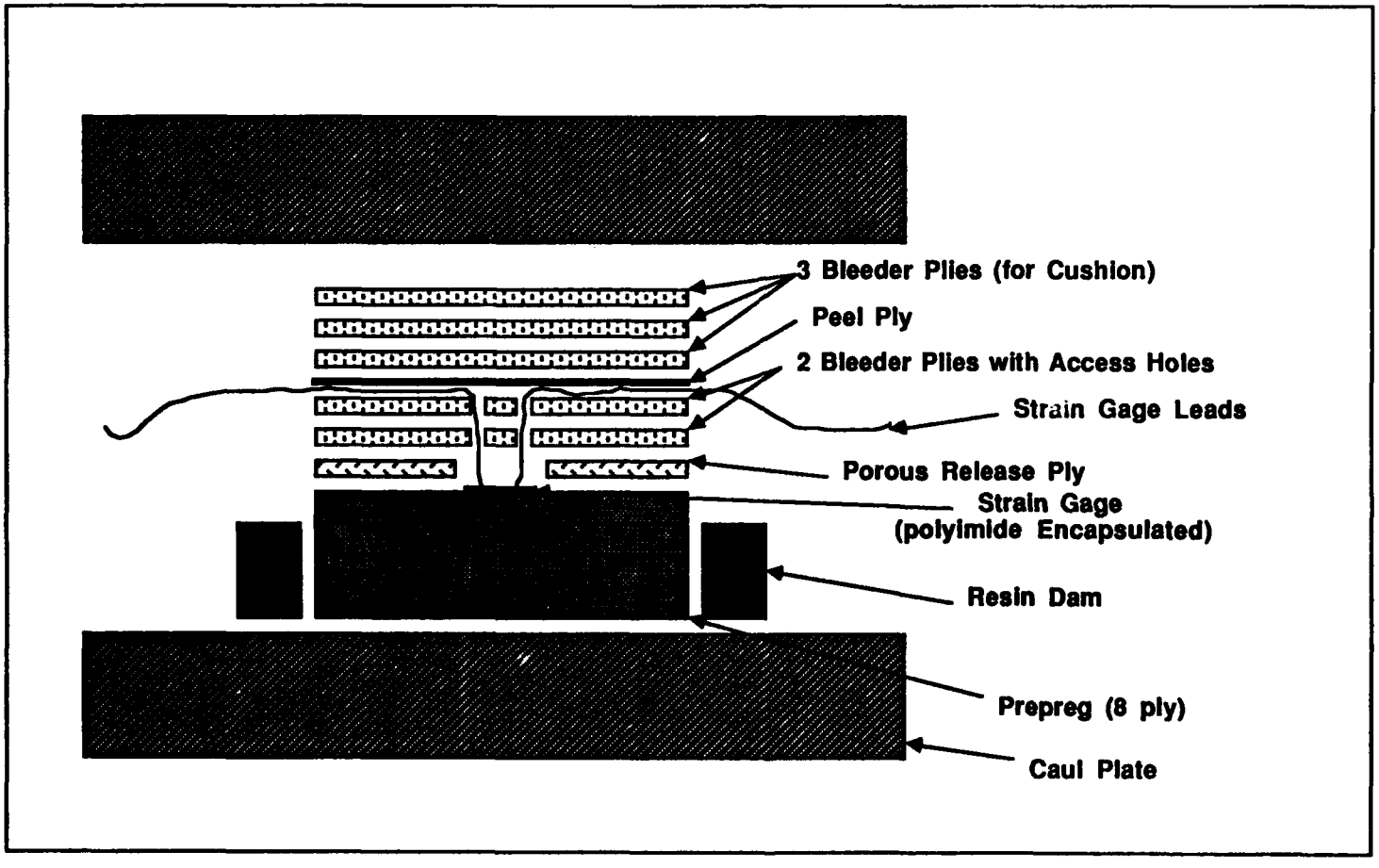

Figure 8. Thermal Strain Experimental Lay-up

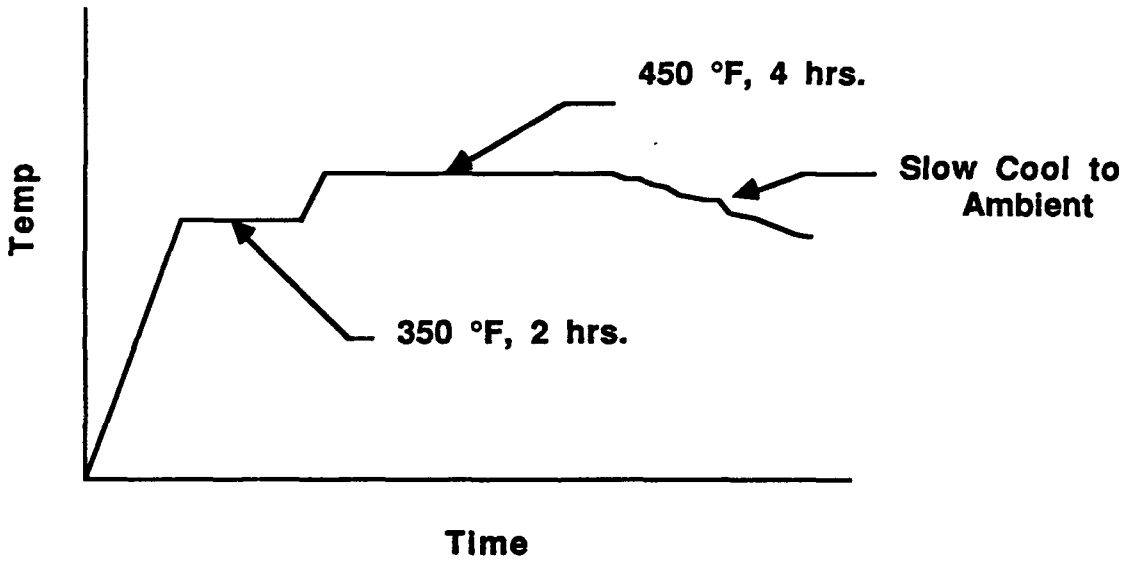

Figure 9. Postcure Cycle for IM6/3100 BMI

3.3. Creep Testing

For input of time-dependent transverse compliance in the viscoelastic model, $[90]_8$ specimens 12.7 mm x 152.4 mm were processed for creep testing according to the intermittent cure schedule in Figure 1. High temperature strain gages (Micro-Measurements WK-06-15BS-120) were bonded with MBOND-610, a high temperature adhesive furnished by Micro-Measurements. Specimens were loaded by dead weight in an ATS Series 2330 creep tester (Figure 10) and strains were recorded throughout the test by an Omega 900 data acquisition system. Type-J thermocouples mounted to the specimens gave a continuous monitor of specimen temperature. A test matrix is given in Table 1.

During creep testing several unforeseen problems were encountered, especially during the high temperature testing. Initially, aluminum end tabs were bonded to the specimen to prevent grip slippage at high temperature. Epon 828 epoxy and curing agent Z were used to bond the end tabs. It was found that the glass transition for the bonding system used was between 110 and 125 °C. At creep temperatures higher than 125 °C, the epoxy bond would flow upon application of the dead weight. Bonding systems with a glass transition higher than 177 °C (the second dwell temperature in the MRC cycle) call for a cure cycle which would have subjected the specimens to a thermal excursion approximating the postcure cycle. Postcured creep data was not of interest for inclusion in equation (10). Therefore, data taken at 177 °C was accomplished by using no end tabs and gripping the specimens tightly with emory cloth between the specimen and the grips.

Additionally, many transverse tensile failures were experienced during load application. The small thickness of the 8-ply specimens coupled with low transverse strengths for intermittently cured specimens and for all specimens at high temperatures dictated that very small loads were applied (9-44 N). During the gripping procedure some bending moments were inevitably applied which were of sufficient magnitude to cause transverse failures.

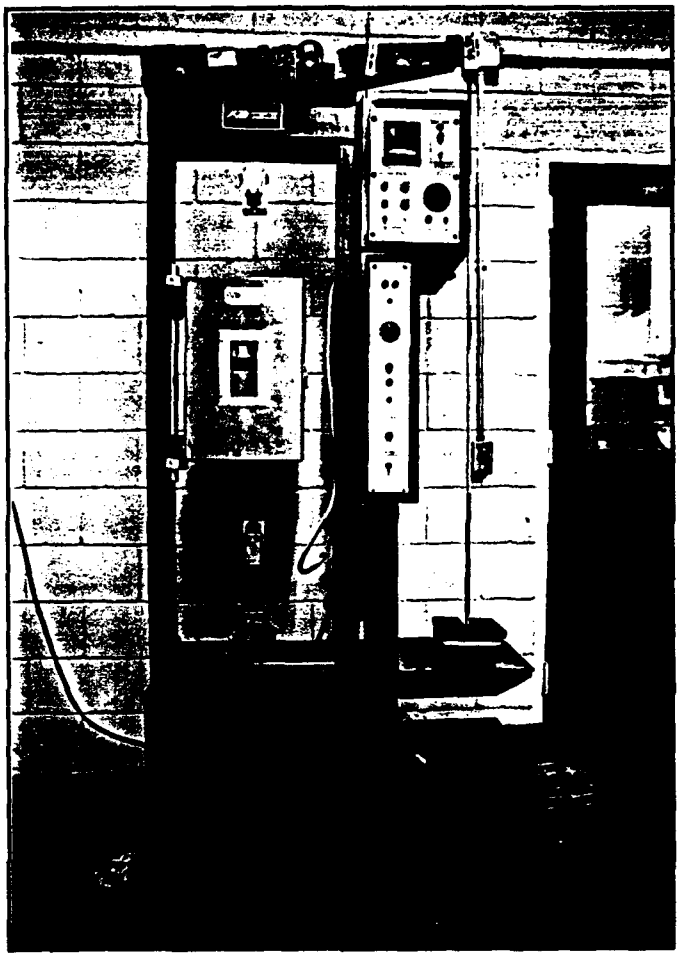

Figure 10. ATS Series 2330 Creep Testing Machine

Table 1. Creep Testing Matrix

Temp (°C)	No. of Spec.	Stress (KPa)	DOC	Failures*
250	1	420	0.98	1
	1	2235	0.98	1
177	2	1118	0.98	
	8	2235	0.98	7
125	2	420	0.39	1
	1	1118	0.98	
	1	2235	0.98	
	1	4470	0.98	
48	3	420	0.39	
	3	1118	0.98	
	2	2235	0.98	

* Failures experienced before or during load application

Also, the load application of the ATS creep machine was quite abrupt. This caused several failures even after successfully gripping the specimens.

Lastly, some strain gage creep may have occurred at 177 °C. This would have caused an overestimation of the viscoelastic stress relaxation of the material at high temperature as was seen in the analytical results.

3.4 Cure Cycle Optimization

Drawing from the experimental results and analytical modelling, several cure cycles were investigated for reducing residual stresses. For each cure cycle investigated the cross-ply curvature, transverse mechanical properties, and degree of cure were obtained. The experimental procedure for these tests has been discussed previously.

4. Results and Discussion

4.1 Mechanical Properties

The longitudinal modulus and strength are shown in Figure 11 at the intermittent cure points. E_L is seen to increase moderately (~20%) throughout the cure cycle. The data indicates no significant changes occurring during cure. This is to be expected since the fibers are the dominant factor in the longitudinal modulus. The fibers are assumed to be unaffected by the cure cycle. In Figure 11(b) the longitudinal strength is seen to increase more dramatically during the cure cycle. An increase of 40% was realized as the specimens became fully cured. Increased matrix strength and better fiber/matrix bonding could account for this increase by helping to distribute the loading. To investigate this phenomena further, the failed longitudinal specimens were analyzed. Figure 12 shows two of the failed specimens. The undercured specimen shows a billowy, mushroom type of failure. Many fibers can be seen which are still continuous from the lower tab to the top. The matrix material exhibits a flaky and powdery type appearance. The lack of complete fiber failure and separation of the top and bottom tabs is indicative of poor load distribution and the matrix flakes are indicative of low matrix strength. The above observations become readily apparent in contrast to the fully cured specimen. Here the fibers have all been completely severed and the matrix material remains well bonded to the fibers after failure. Observations of transverse tension failure surfaces in Figure 13 show that for the undercured specimen many bare fibers have been pulled out during failure. This is indicative of poor fiber/matrix adhesion as well as low strength of the matrix. Observations of the fully cured specimen show essentially no dangling fibers and a clean failure surface.

The major Poisson's ratio was found to decrease from 0.37 to 0.29 during the cure cycle as seen in Figure 14. This decrease could be predicted from a rule of mixtures

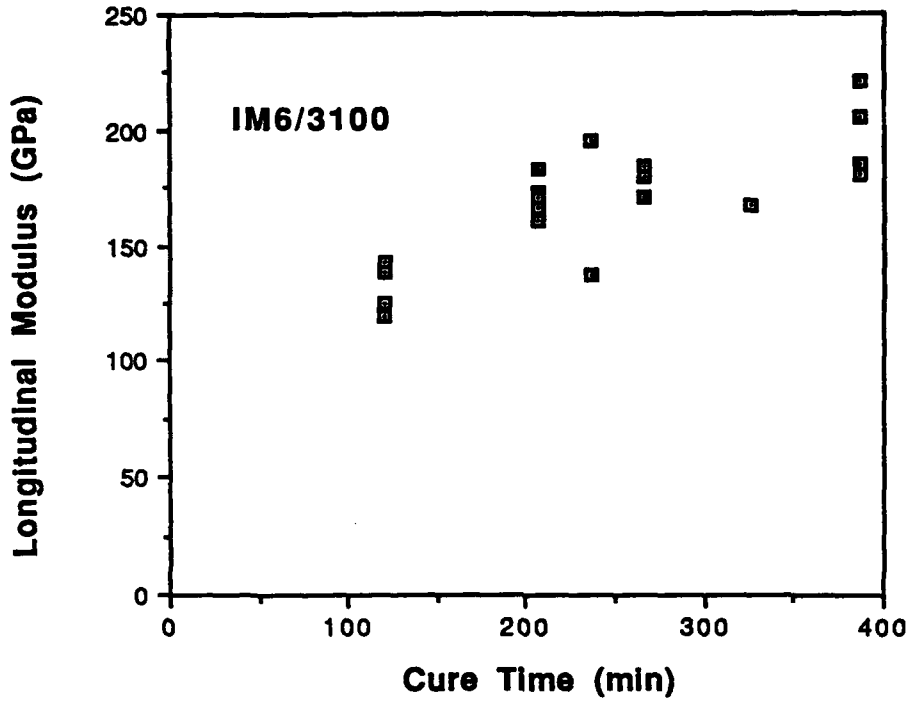

(a)

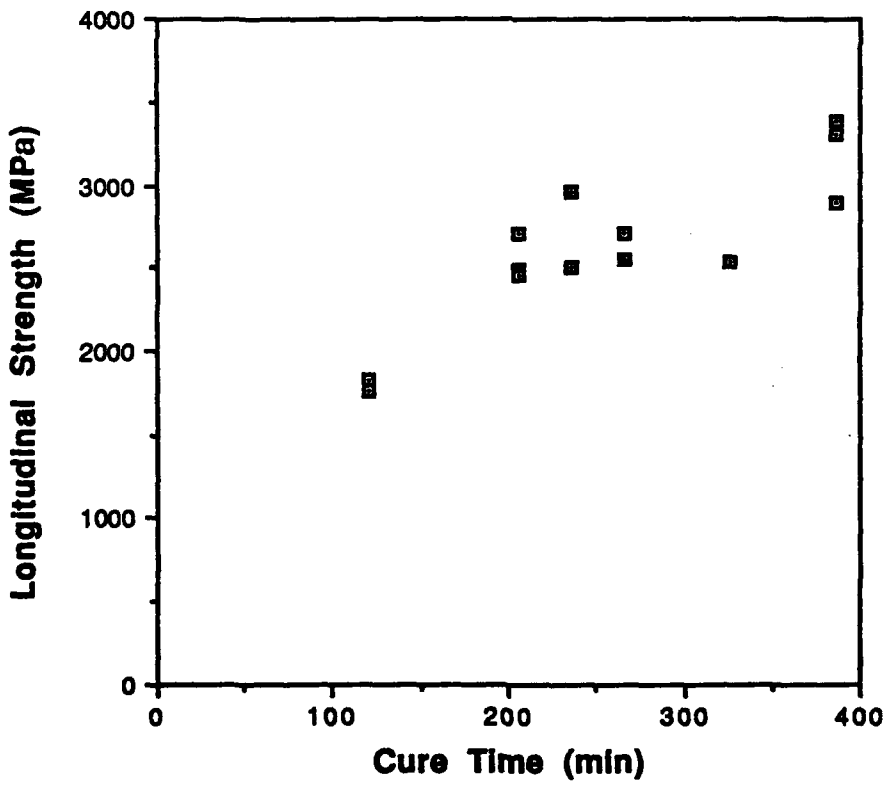

(b)

Figure 11. Longitudinal Mechanical Properties vs. Cure Time of Intermittent Cure Specimens

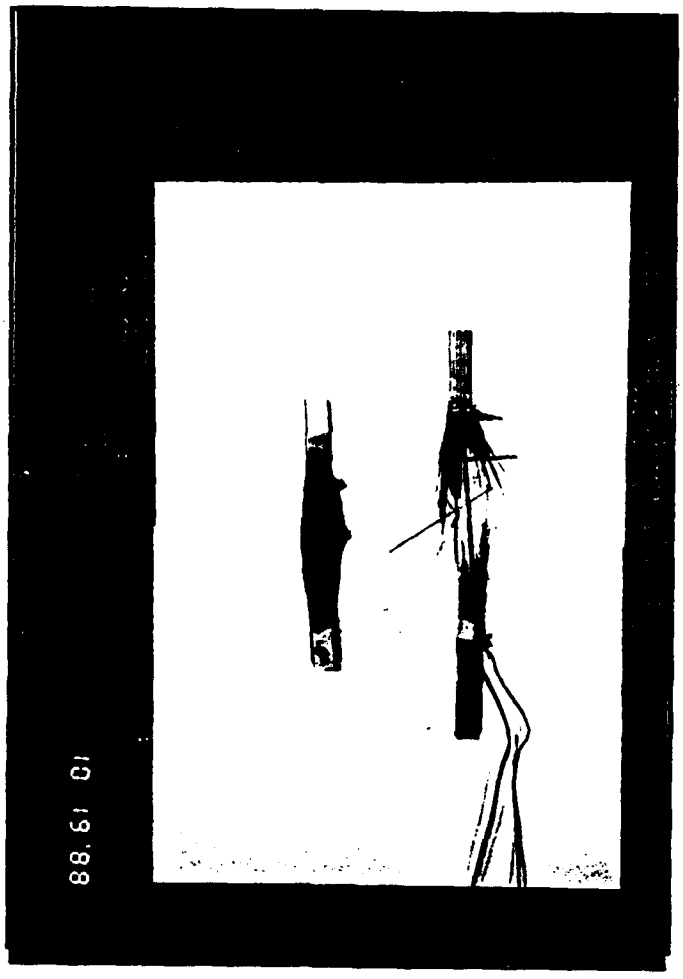

Figure 12. Failed O° Tension Specimens

Left Spec: DOC = 0.229
Right Spec: DOC = 0.980

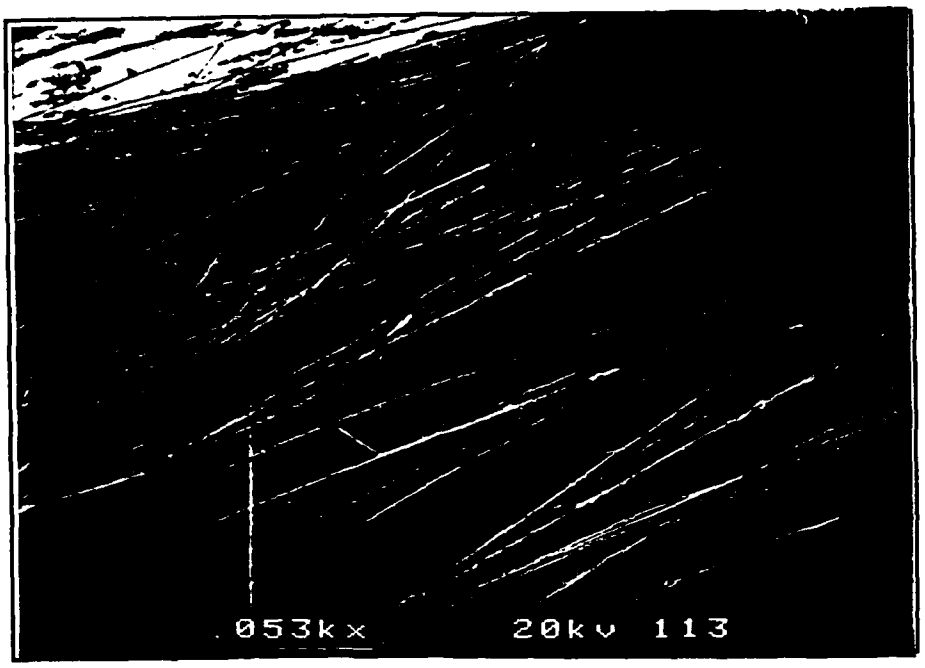

(a)

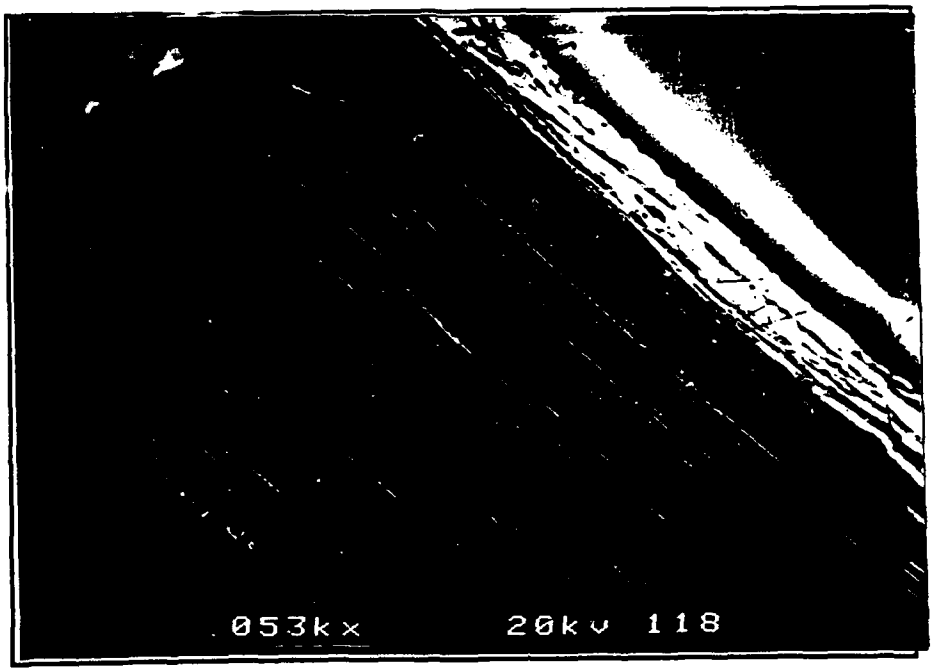

(b)

Figure 13. 90° Tension Failure Surfaces
(a) Undercured Specimen DOC = 0.229
(b) Fully cured Specimen DOC = 0.956

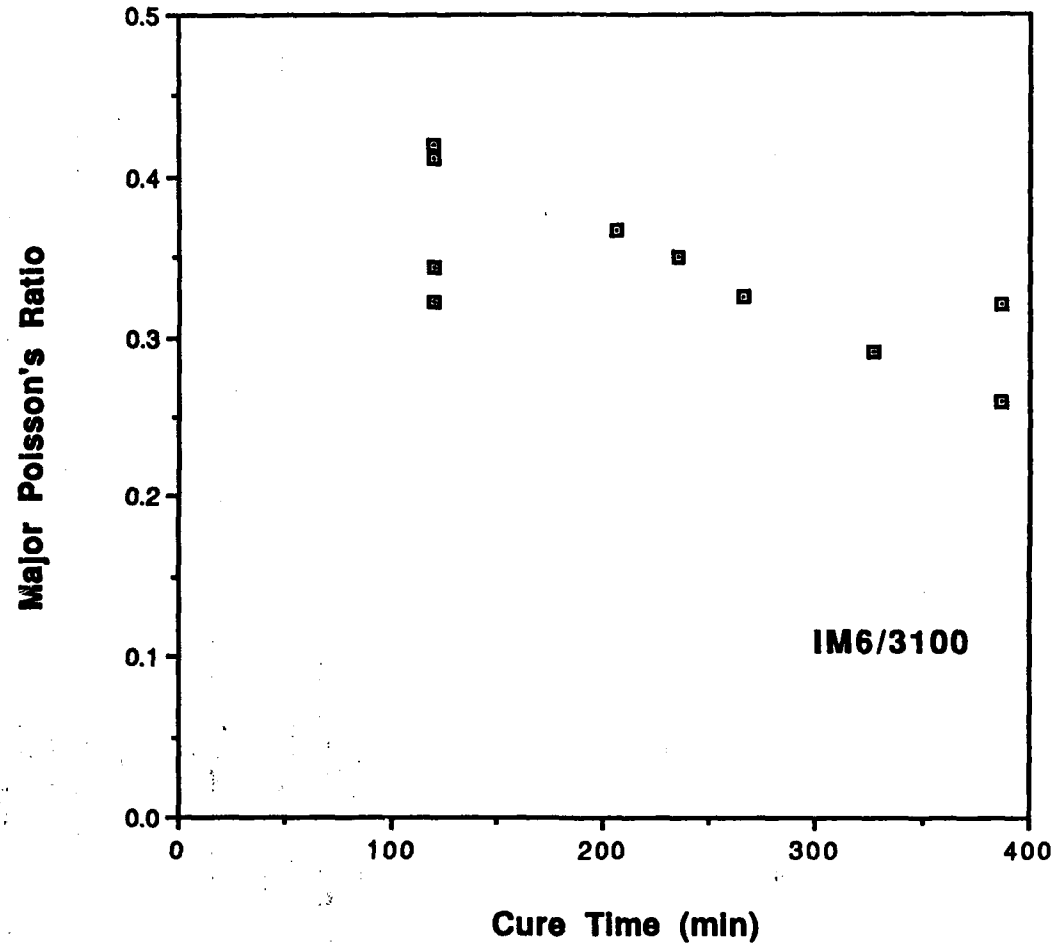

Figure 14. Major Poisson's Ratio vs. Cure Time of Intermittent Cure Specimens

equation while taking into account the change in Poisson's ratio of the matrix and the change in fiber volume content during the cure cycle. In this case the rule of mixtures gives

$$\nu_{LT}(c) = v_f\nu_f + v_m\nu_m(c) \tag{19}$$

In equation (19) c is the degree of cure (0 = uncured, 1 = fully cured). Initially, $\nu_m(0) \approx 0.5$ and when fully cured $\nu_m \approx 0.35$. Assuming a change in fiber volume content of 60% to 70% and $\nu_f = 0.25$, equation (19) yields:

$$\nu_{LT}(0) = 0.35$$

$$\nu_{LT}(1) = 0.28$$

The transverse modulus and strength both show significant changes during the cure cycle as evidenced in Figure 15. Since the matrix material is dominant in the transverse direction, the changes that the matrix material is experiencing during cure is reflected in these properties. The transverse modulus, E_T, was found to increase rapidly after the initial dwell period before reaching its fully cured value. For the first intermittent cure point the transverse strength was too low to allow an E_T calculation. The transverse strength is seen to increase monotonically until reaching the fully cured value. It is interesting to note that the transverse strength has not reached a maximum value at the end of the MRC cycle. If the cure time were to be extended a further increase in strength might be obtained. And indeed a postcure cycle is recommended for the material. After postcure an increase of 32% was realized in the transverse strength. Another important observation to be made is that the transverse strength does not develop as quickly as the modulus during the cure cycle. This was evident in the first intermittent cure point when the strength was too low to allow determination of the modulus.

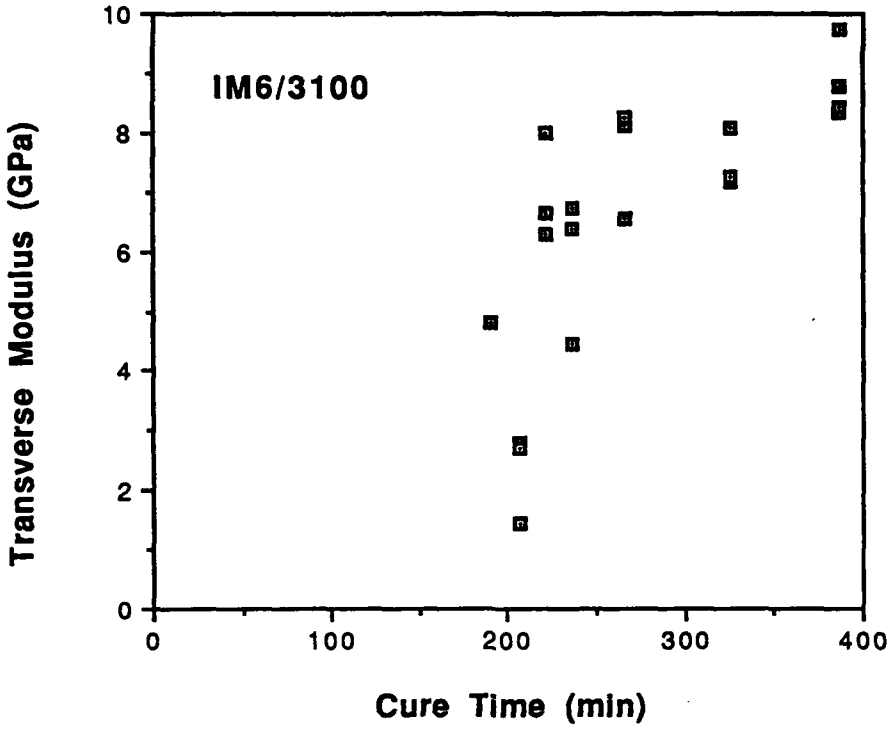

(a)

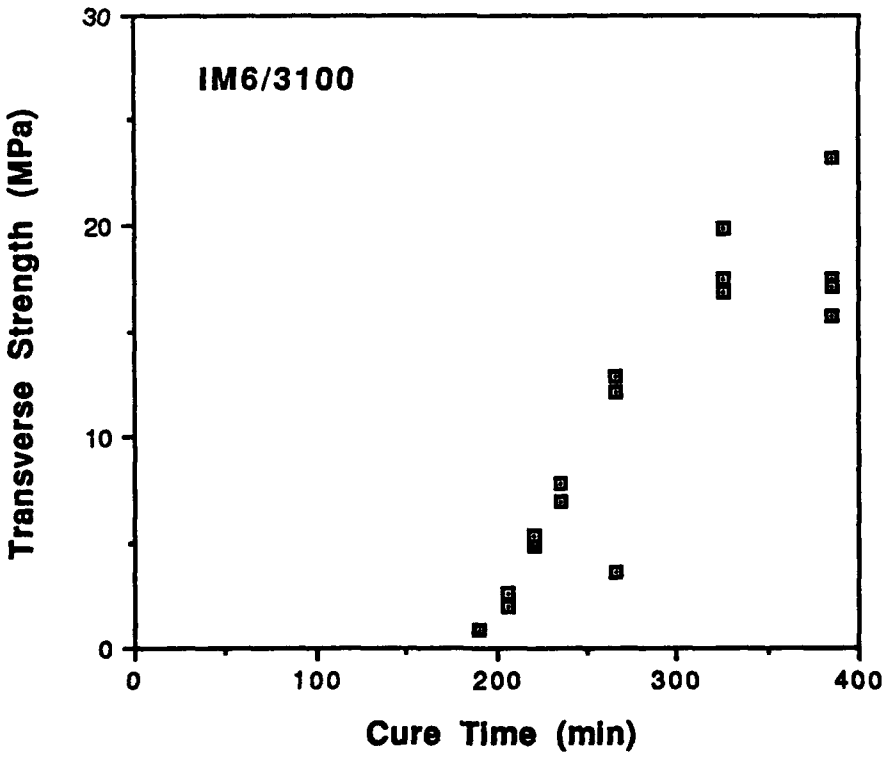

(b)

Figure 15. Transverse Mechanical Properties vs. Cure Time of Intermittent Cure Specimens

4.2 DSC Testing

From equation (18) the degree of cure was calculated for each of the intermittently cured specimens. The results are plotted in Figure 16. During the initial dwell period the degree of cure is quite low. Upon heat up to the second dwell temperature the reaction rate increases significantly and the degree of cure increases rapidly. After one to two hours dwell the cure is nearly complete. Upon analyzing Figure 16 it was found that a large grouping of the data was above $c = 0.8$ when cure was nearing completion. Therefore another intermittently cured specimen was run to obtain more data below $c = 0.8$. A specimen with $c = 0.39$ was obtained by stopping the cure cycle at the beginning of the second dwell.

With the data obtained from the degree of cure study, the dependence of mechanical properties on degree of cure was investigated. Figures 11 and 15 were replotted against degree of cure in Figures 17 and 18 respectively.

The longitudinal properties of the laminate increase with increasing degree of cure as shown in Figure 17. The reasons for this trend have been discussed previously. Some researchers [18] have reported no significant changes in longitudinal properties with degree of cure. However, their data has been restricted to degrees of cure of 0.6 or more. When analyzing the full range of cure state ($c = 0$ to $c = 1$) the trend in longitudinal properties is readily apparent. Thus, the fiber properties will be the dominant factor in longitudinal properties, but the cure cycle effects on matrix strength and fiber/matrix adhesion will also affect laminate longitudinal properties significantly.

Analysis of the transverse strength and modulus in Figure 18 show some quite remarkable results. The degree of cure of the resin must be quite high before the transverse properties of the laminate begin to develop. In addition it is quite evident that the transverse strength does not develop as fast as the modulus as cure progresses. Significant changes in strength of the resin are occurring in the final stages of cure where $c > 0.9$. Whereas the

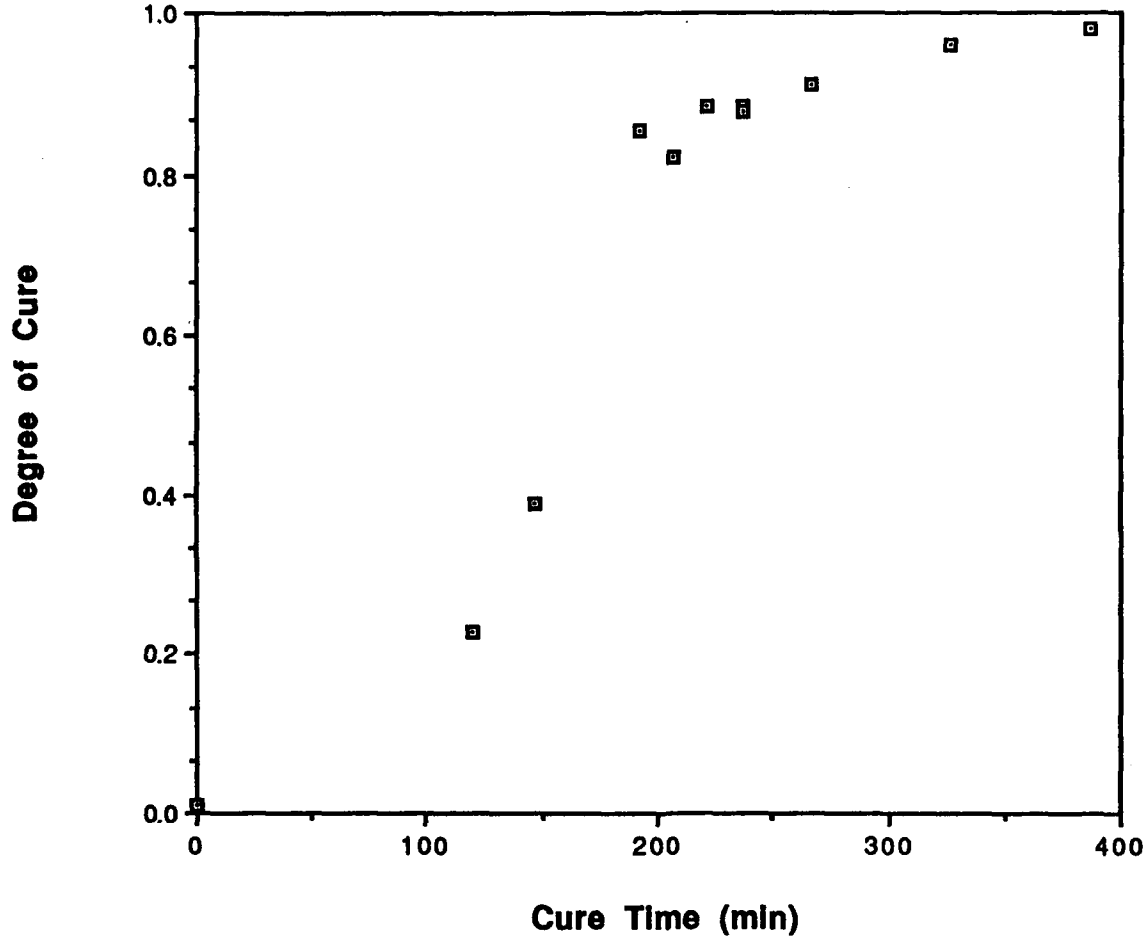

Figure 16. Degree of Cure Measured from DSC Testing of Intermittent Cure Specimens

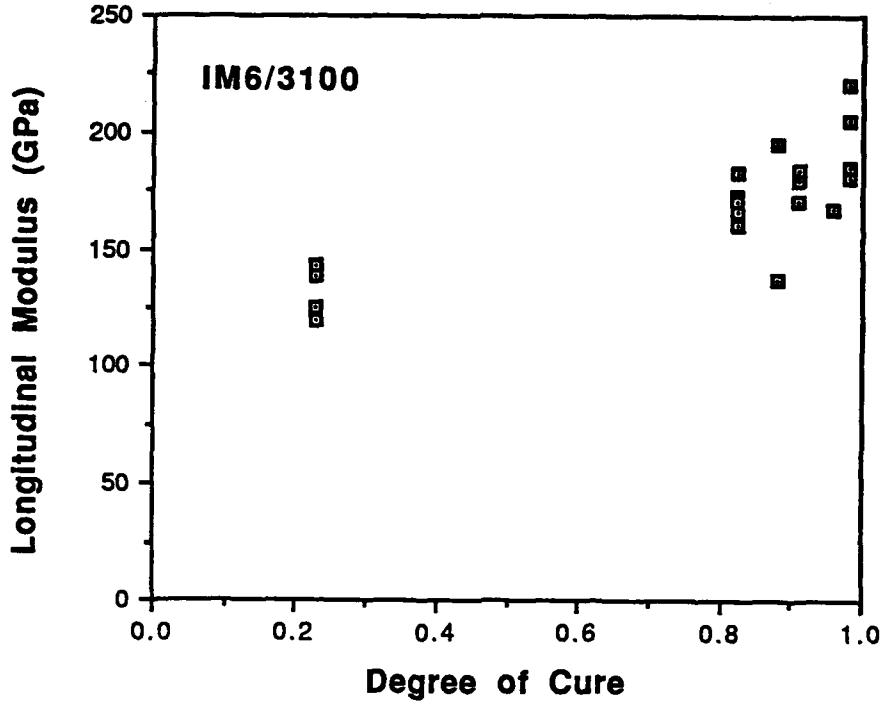

(a)

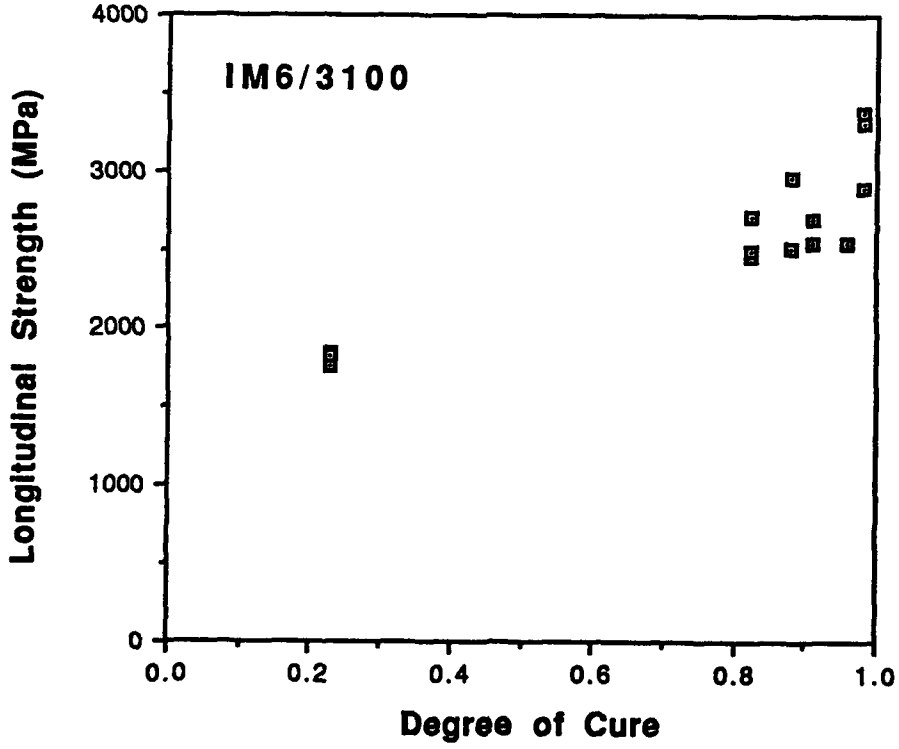

(b)

Figure 17. Longitudinal Mechanical Properties vs. Degree of Cure of Intermittent Cure Specimens

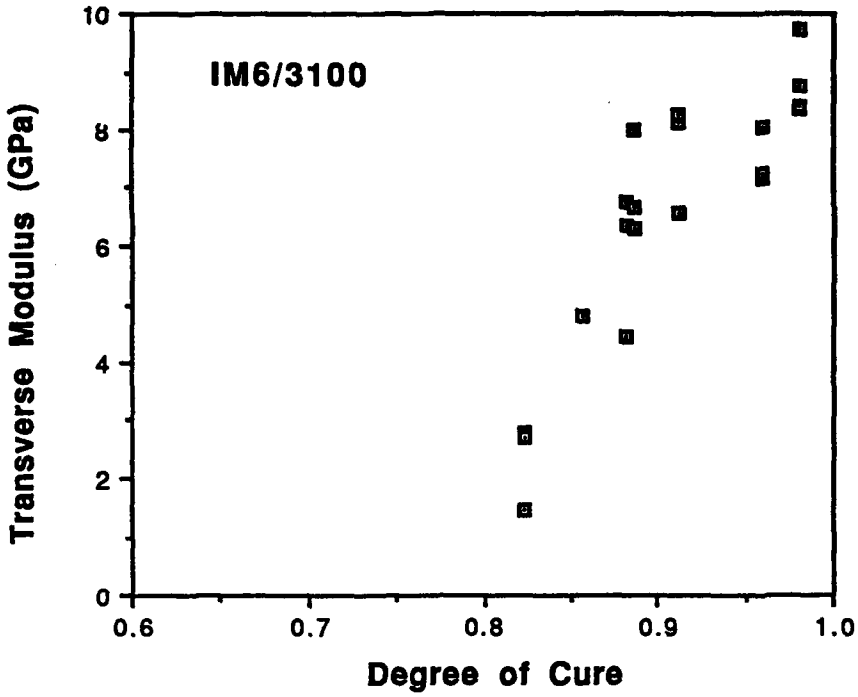

(a)

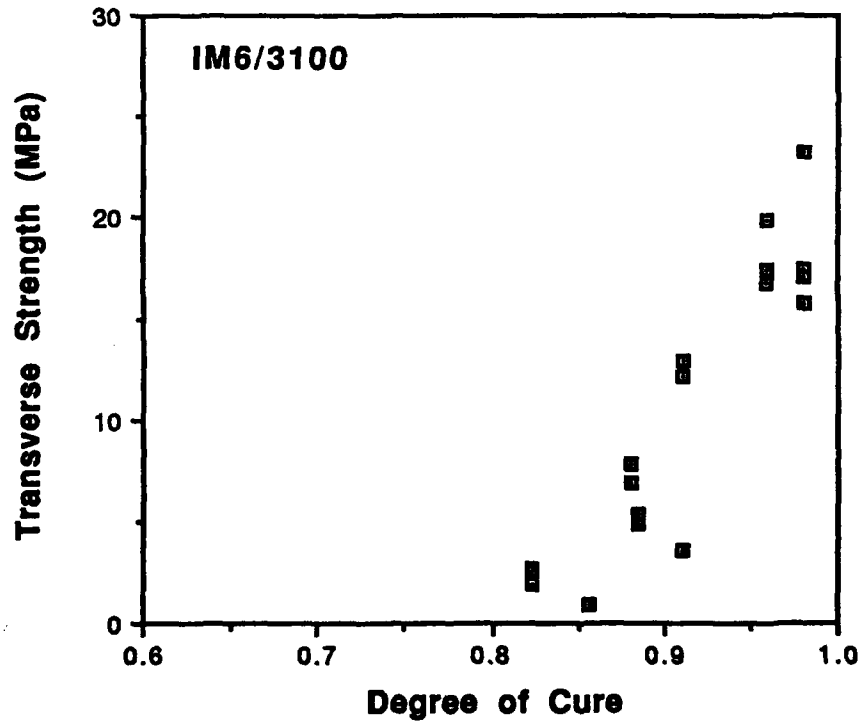

(b)

Figure 18. Transverse Mechanical Properties vs. Degree of Cure of Intermittent Cure Specimens

resin modulus is not affected to the same degree by the strength of bonding, but rather the degree of entanglement. As curing occurs the polymer chains become entangled and finally "set", after which the strength of the resin is developed.

Having analyzed the mechanical property development during the cure cycle and the cure state of the intermittently cured specimens, the thermal strains were obtained experimentally for inclusion in equation (7).

4.3. Thermal Strains

Figure 19 is a representative result for these tests in which one of the undercured specimens was monitored. During heat-up resin flow is taking place as well as chemical shrinkage. Thus, the results during heat-up are difficult to analyze. However, the cool-down strains are easily obtained from the data. The longitudinal strains are seen to be quite small and of opposite sign compared to the temperature differential. Thus, during cool-down a small expansional strain occurred in the longitudinal direction. The transverse thermal strains were taken as

$$e_T = \varepsilon_{RT} - \varepsilon_{BCD} \tag{20}$$

where RT signifies room temperature and BCD is the beginning of cool-down. A summary of the thermal strain testing is given in Figure 20. The transverse thermal strain is plotted versus the cure time. The data indicates that the thermal strain remains relatively constant throughout the cure cycle. The results of DSC testing of the thermal strain specimens (Figure 21) indicated a clustering of data above c = 0.8, however the specimen at a degree of cure of 0.38 did not show a significant change in transverse thermal strain. Therefore, in the subsequent analysis the thermal strains were assumed constant during the cure cycle.

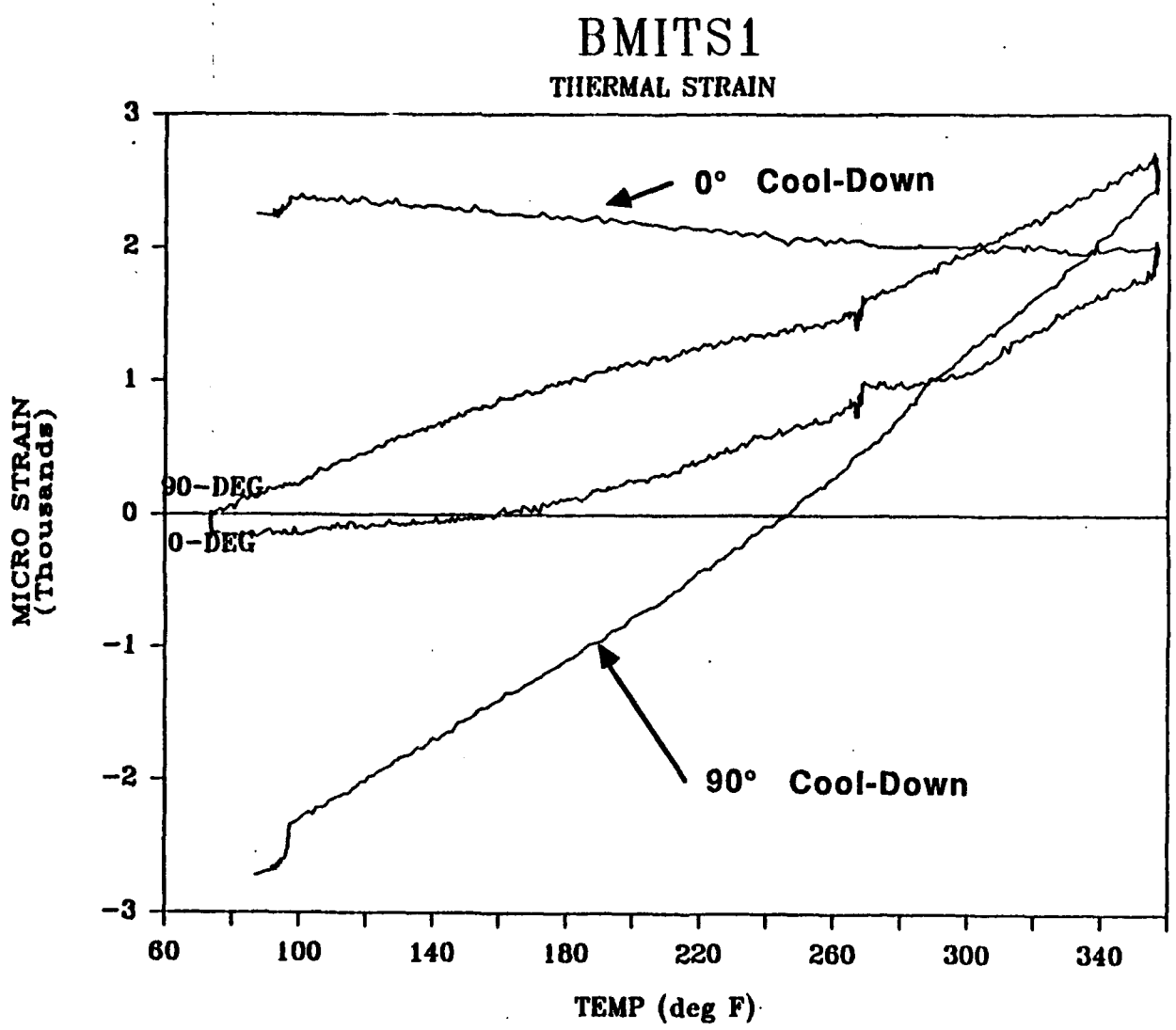

Figure 19. Thermal Strains During MRC Cycle (IM6/3100)

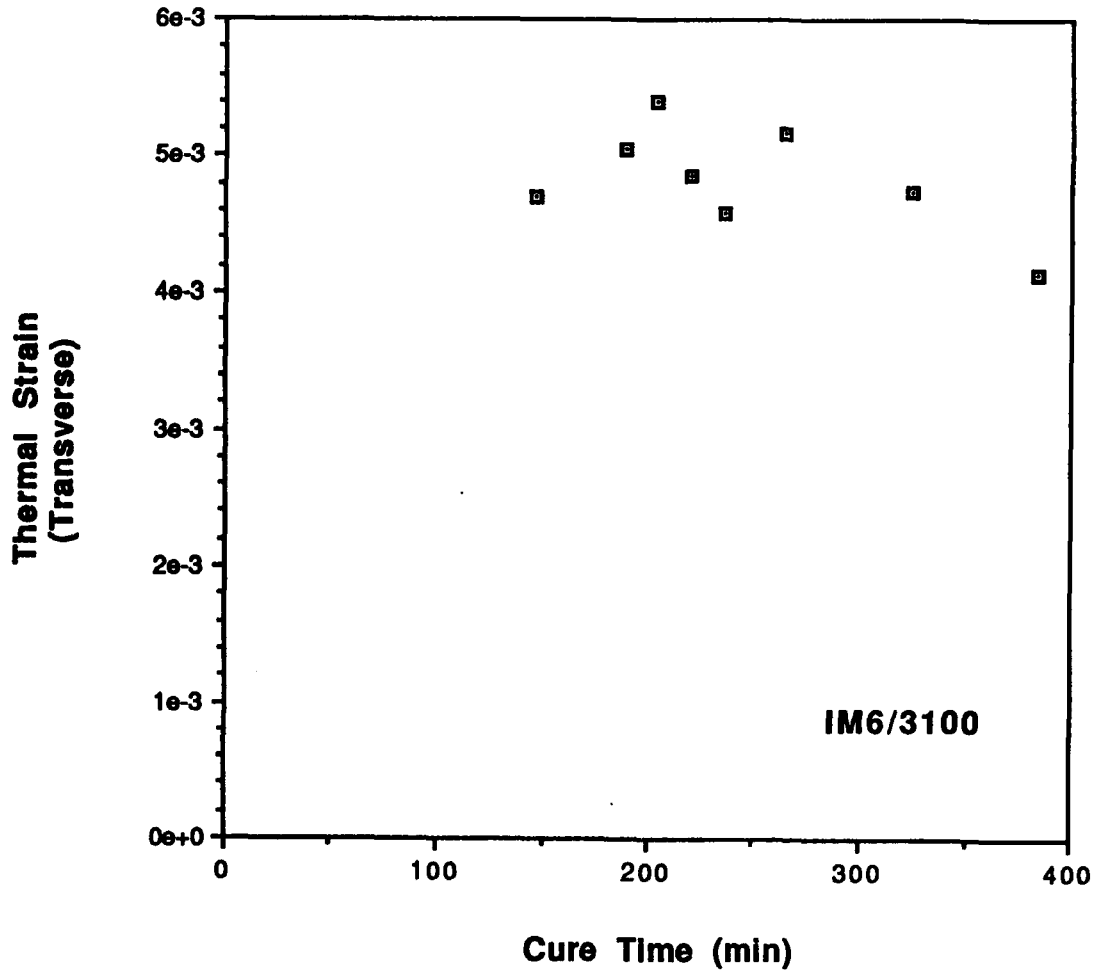

Figure 20. Thermal Strain vs Cure Time for Intermittent Cure Specimens

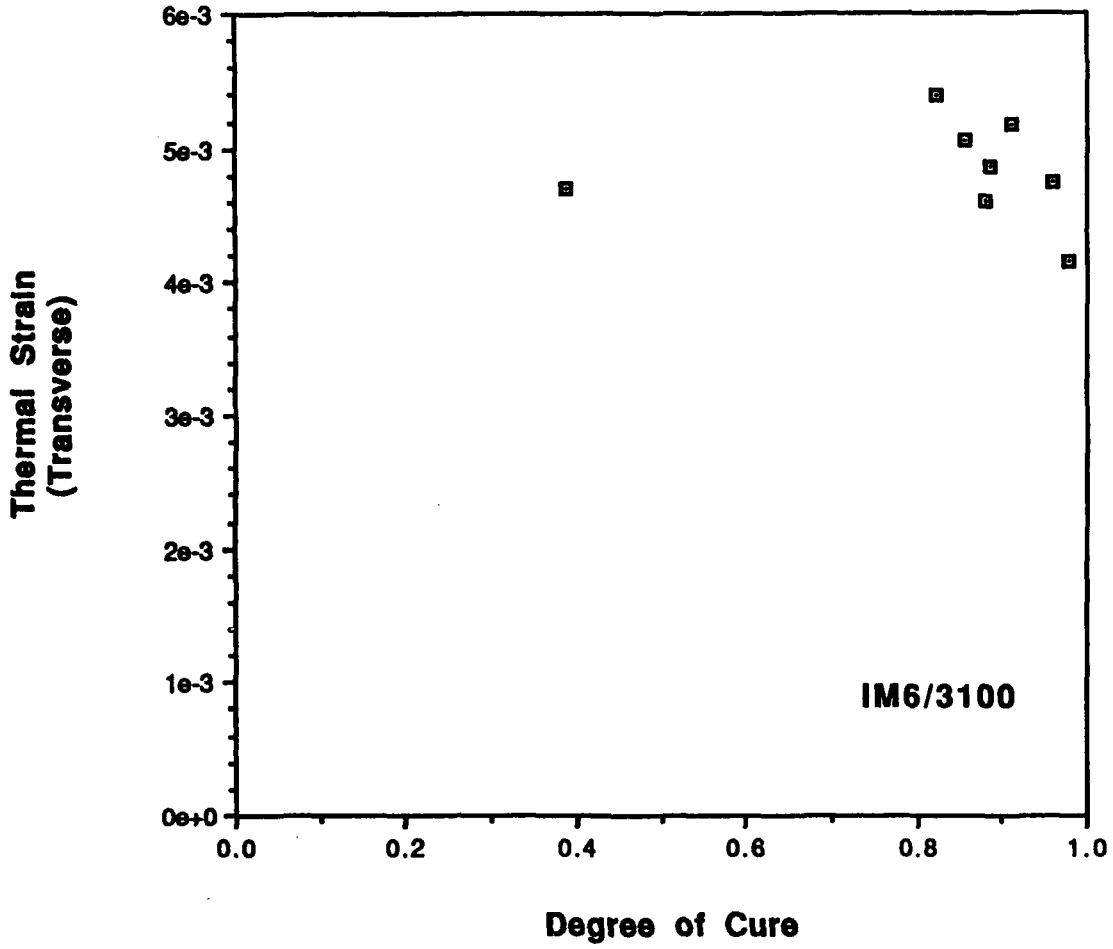

Figure 21. Thermal Strain vs Degree of Cure of Intermittent Cure Specimens

4.4. Elastic Analysis

Drawing upon the results of the mechanical property and thermal strain testing the dimensionless curvature was modeled by equation (7). Table 2 summarizes the input data for the elastic model for the intermittently cured specimens. The predicted dimensionless curvature is plotted versus the experimental data in Figure 22. Within the experimental scatter equation (7) predicts the curvature induced during cure except for two groups of data (7A, 8A) in which the measured curvature was significantly less than the predicted value. These two groups of specimens were analyzed for evidence of transverse cracking which was believed to have relieved some of the residual stresses and lowered the measured curvature. X-ray radiography specimens were prepared by immersion is di-iodobutane (DIB) penetrant. DIB penetrant is opaque to X-rays. Therefore, transverse cracks will appear as solid lines on an X-ray image. Both groups of data, 8A and 7A, showed significant transverse cracking as evidenced in Figure 23. The crack densities for specimens in groups 8A and 7A were measured as 31 and 25 cracks/inch respectively. These two groups of data experienced transverse cracking due to the lag in transverse strength development compared to the transverse modulus during the cure cycle. Both groups of specimens were cured until the early stages of the four hour second dwell (45 minutes for 8A and 75 minutes for 7A into the second dwell point) and had degrees of cure of 0.856 and 0.886 respectively. Referencing Figure 18 the transverse strength is quite low at these cure states while the transverse modulus has developed sufficiently to allow residual stresses to develop. During cool-down the residual stresses build up until the transverse strength of the laminate is exceeded and transverse cracks are induced. Specimens cured longer than these two groups have transverse strengths which are greater than the residual stresses induced and thus, no transverse cracking occurs. Specimens which are cured less than 7A and 8A show no signs of transverse cracking because the modulus is quite low and therefore the residual stresses are low. Figure 24 is a vivid

TABLE 2. Input Parameters for Equation (7)
[Mean Exp. Values]

CURE TIME (min)	ν (major)	E (E_T/E_L)	$e_L - e_T$ [$\mu\varepsilon$]
120	0.370	0.009	2512
191	0.366	0.026	4539
206	0.351	0.013	4539
221	0.340	0.038	4539
236	0.326	0.032	4539
266	0.291	0.042	4539
326	0.321	0.041	4539
386	0.290	0.048	4539

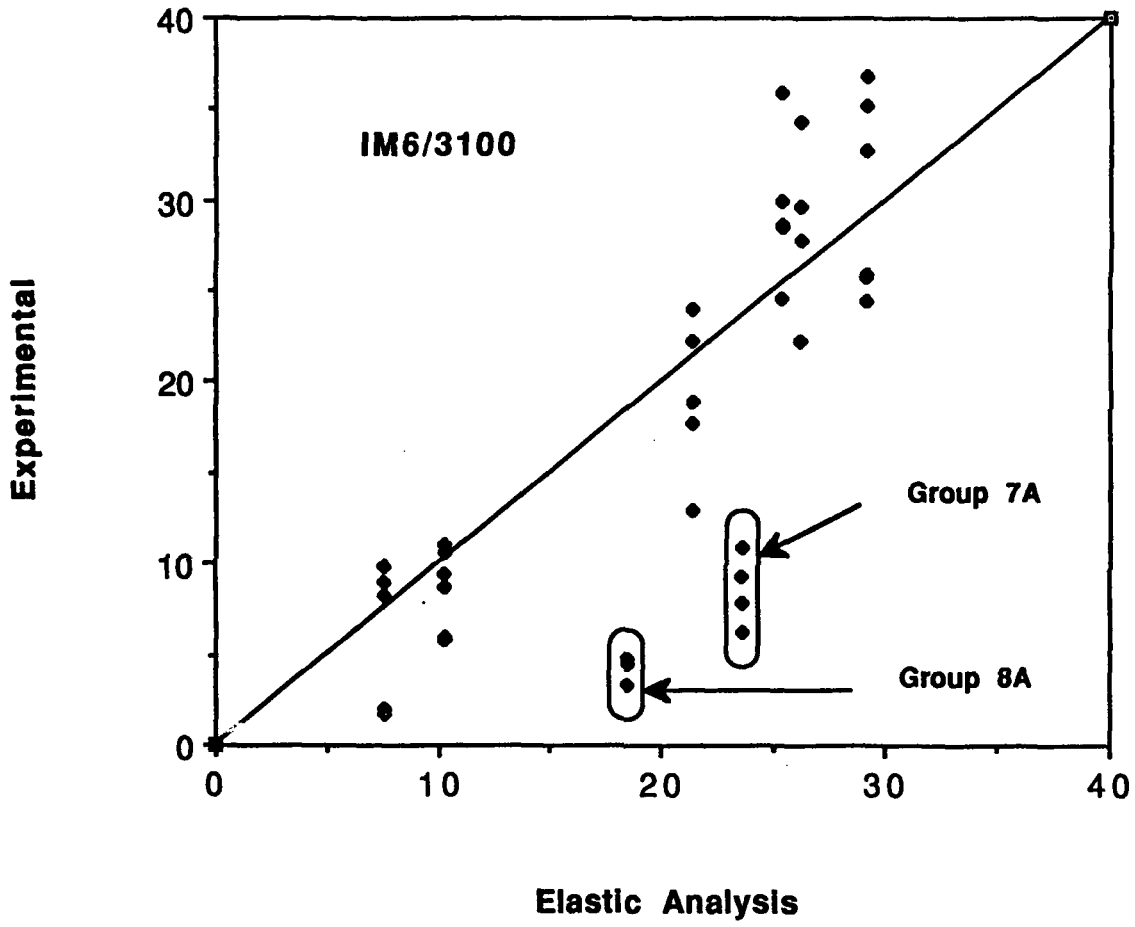

Figure 22. Dimensionless Curvature of Intermittent Cure Specimens Elastic Model Prediction vs. Experimental Data

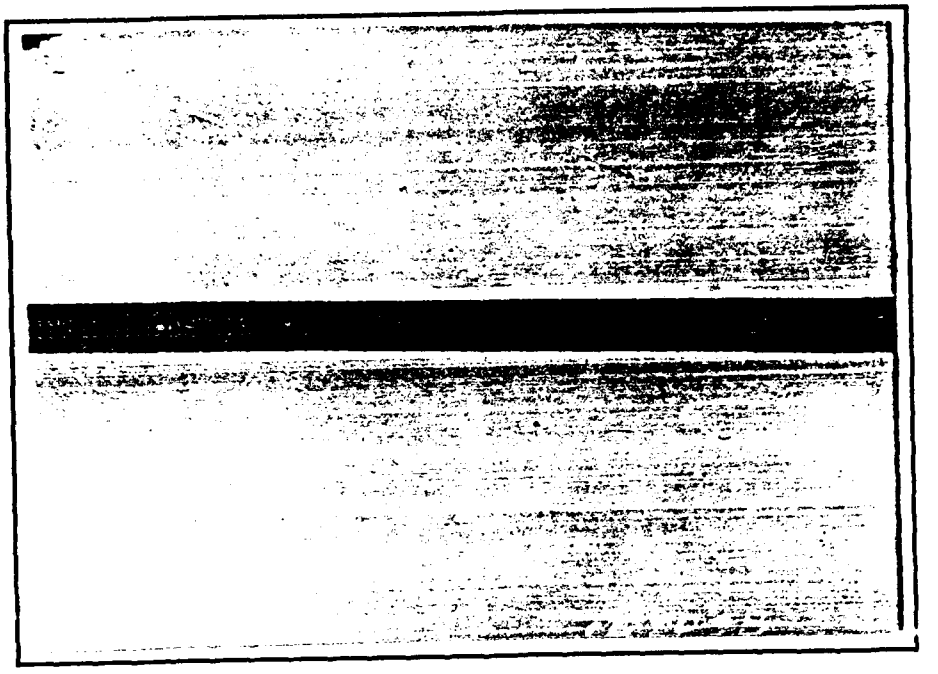

(a)

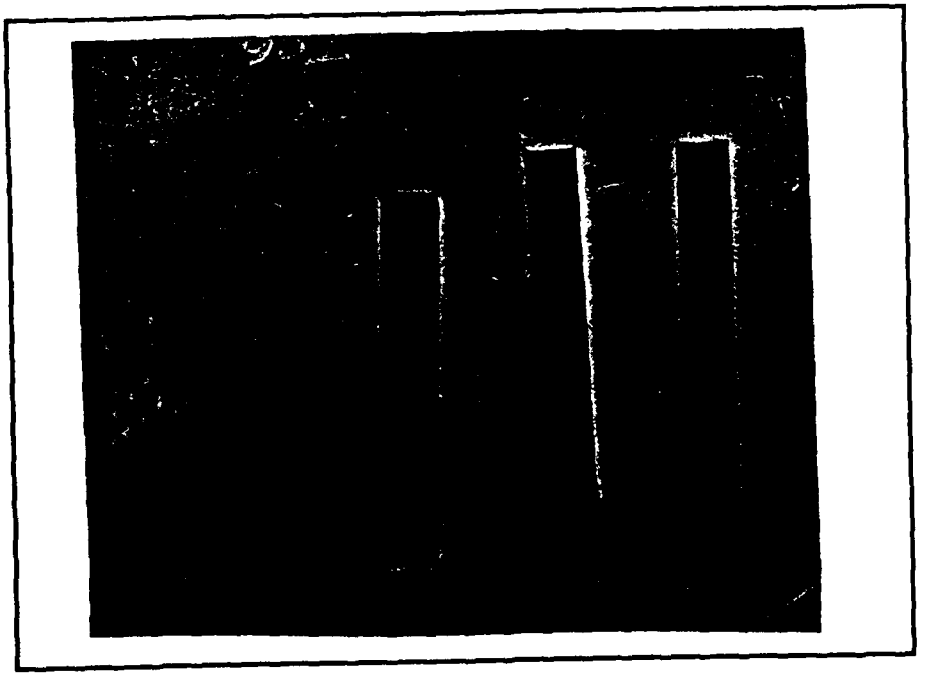

(b)

Figure 23. X-ray Radiographic Images Showing Transverse Cracking after Processing

(a) Specimen 7A-1
(b) Specimen 8A-2

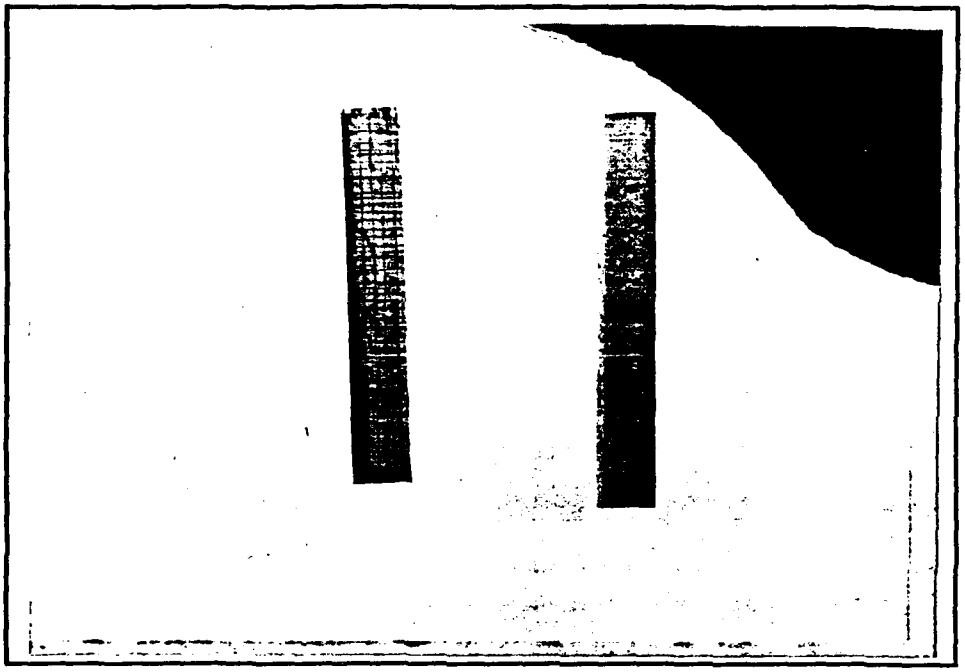

Figure 24. Transverse Cracking Assessment in Intermittent Cure Specimens (Small Variations in Cure Cycle can have Deleterious Effects on Part Quality)

representation of how important the cure cycle parameters are on the part quality and, ultimately, the mechanical properties . Specimen 2A was cured thorough the full MRC cycle and showed no signs of transverse cracking. Thus, a slight change in the cure cycle of a material (in this case the dwell time), can have deleterious effects on the processed material.

4.5. Chemical Shrinkage

Equation (7) does not account for chemical strains in the curvature development. Since chemical shrinkage strains occur at high temperatures (the cure temperature) when the modulus is low and stress relaxation can take place, it was believed that their contribution to residual stress development is negligible. A $[O_4/9O_4]_T$ 12.7 mm x 152.4 mm specimen was layed up and placed on a base plate in an oven chamber with a glass viewing port. The specimen was cured, unconstrained (applied pressure = atmospheric), through the full MRC temperature cycle. The curvature development was monitored through the viewing port during the cure cycle. If chemical shrinkage plays a roll in the residual stress development, curvature should have been induced during the second dwell period. No curvature development was seen during the second dwell. Unfortunately, the curvature development during cool-down was also negligible due to lack of consolidation between plies. Delamination was evident throughout the specimen after processing. Therefore, the results were inconclusive.

Chemical shrinkage effects can also be analyzed from postcure experiments on the intermittently cured specimens. Since additional chemical strains would occur in the undercured specimens, additional curvature can be induced.

4.6. Postcure

Dimensionless curvature and weight loss results for postcure are given in Figure 25. The horizontal axis is plotted as initial degree of cure, the degree of cure obtained from DSC testing after the intermittent MRC cycle. The curvature is seen to increase after postcure for all specimens. A number of factors could increase the curvature after postcure. Firstly, any additional chemical shrinkage which takes place will contribute to the increases in curvature. Secondly, the loss of moisture reduces the swelling strains in the laminate. Also, increasing the transverse modulus after postcure will cause additional curvature to be induced (see equation 7).

From Figure 25 the moisture loss is seen to be especially prevalent in the undercured specimens. For example the weight loss for c = 0.229 specimens was 0.535% after postcure. For the fully cured specimens the weight loss was 0.142%.

To ascertain the effect of increased transverse modulus after postcure, nine $[9O]_8$ 12.7 mm x 152.4 mm postcured specimens were mechanically tested according to section 3.1.2.2 to obtain the transverse modulus after postcure. Once this data was obtained the increase in curvature due to the change in transverse modulus was predicted using equation (7).

Table 3 shows the results of this testing and analysis. The change in curvature after postcure can be predicted when accounting for the changes in transverse modulus. Additionally, the moisture loss during postcure increases the experimental curvature beyond that predicted by equation (7). The small differences between the predicted and experimental curvature can be accounted for in this manner. The data at c = 0.804 showed some transverse cracking which reduced the experimental curvature from the prediction.

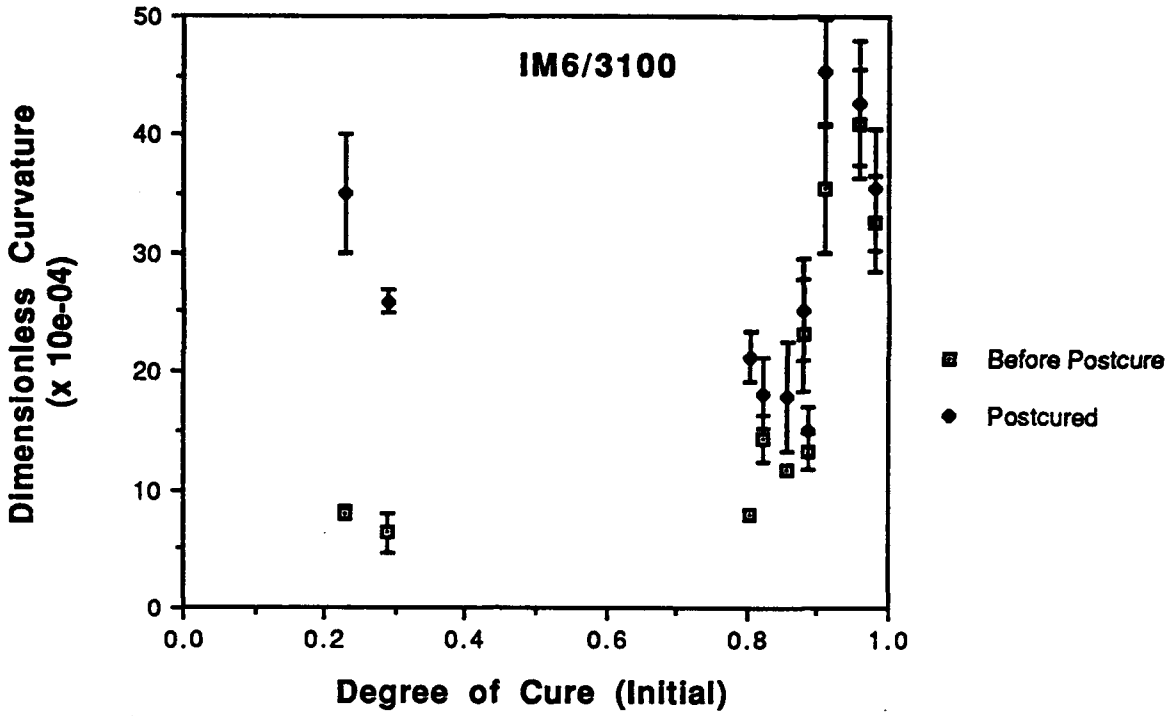

(a)

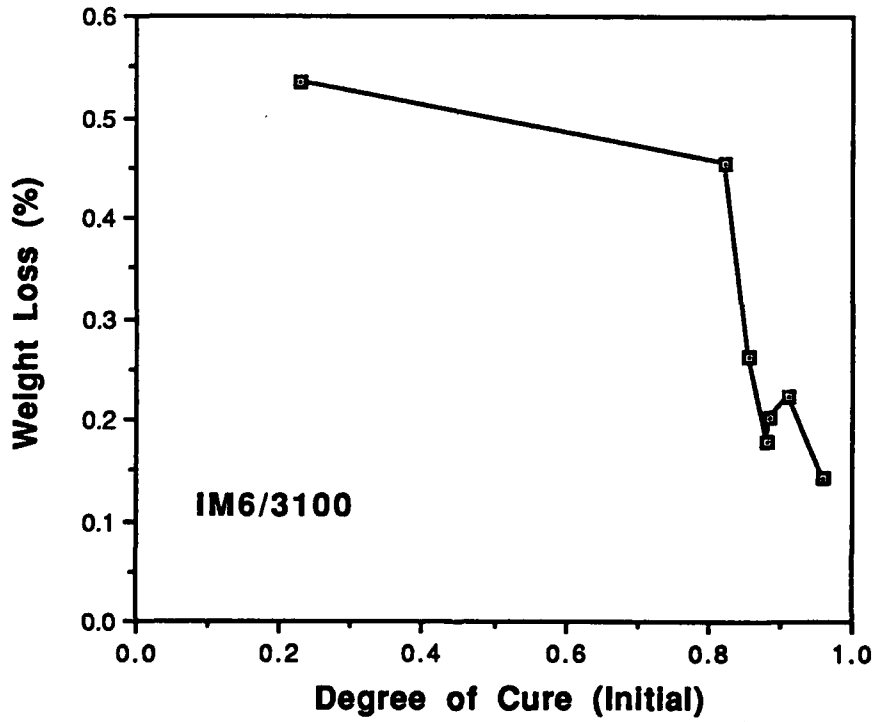

(b)

Figure 25. Dimensionless Curvature (a) and Weight Loss (b) After Postcure of Intermittent Cure Specimens

Table 3: Change in Curvature Predicted after Postcure

Degree of Cure	ΔE (GPa)	Δtk (Analysis)	Δtk (Experimental)
0.804	4.924	15.213	13.261
0.911	1.662	2.960	3.600
0.980	1.083	2.060	3.090

4.7. Viscoelastic Modeling

Stress relaxation at high temperature could be used as an optimization technique to reduce residual stresses during processing. The viscoelastic effects of polymeric resins become more prominent at elevated temperatures, while at room temperature their behavior is predominantly elastic. Equation (10) was used to model the curvature development during cool-down from the cure temperature.

The creep data was analyzed to obtain the transverse time-dependent compliance and the shift factor for input in the viscoelastic model. The transverse compliance master curve and the shift factor are plotted in Figures 26 and 27 respectively. As can be seen from Figure 26, the creep data at high temperature is sparce. Confirmation data at 177 °C and data between 126 and 177 °C is needed. To the author's knowledge there is no creep data available for the IM6/3100 BMI material.

The reduced creep data and other mechanical properties of interest were included in equation (16) and dimensionless curvature obtained during cool-down. The values used for the input variables are given in Table 4. The curvature induced during cool-down at 5.6 °C/min (10 °F/min) is shown in Figure 28.

During the initial stages of cool-down the curvature development is small due to stress relaxation. As the temperature is reduced and the material cools down, viscoelastic effects become negligible and the curvature development is linear elastic to room temperature. The curvature predicted by equation (16) at room temperature was compared to the elastic prediction of 29.43 and experimental of 31.18 x 10e-04. The obvious explanation for this discrepancy is that the high temperature creep data is overpredicting the actual creep experienced by the material. Strain gage and gage bond creep could account for this. But more importantly since the residual stresses (dimensionless curvature) have been shown to be accurately predicted by elastic analysis, it is believed that viscoelastic effects play a minor role in residual stress development.

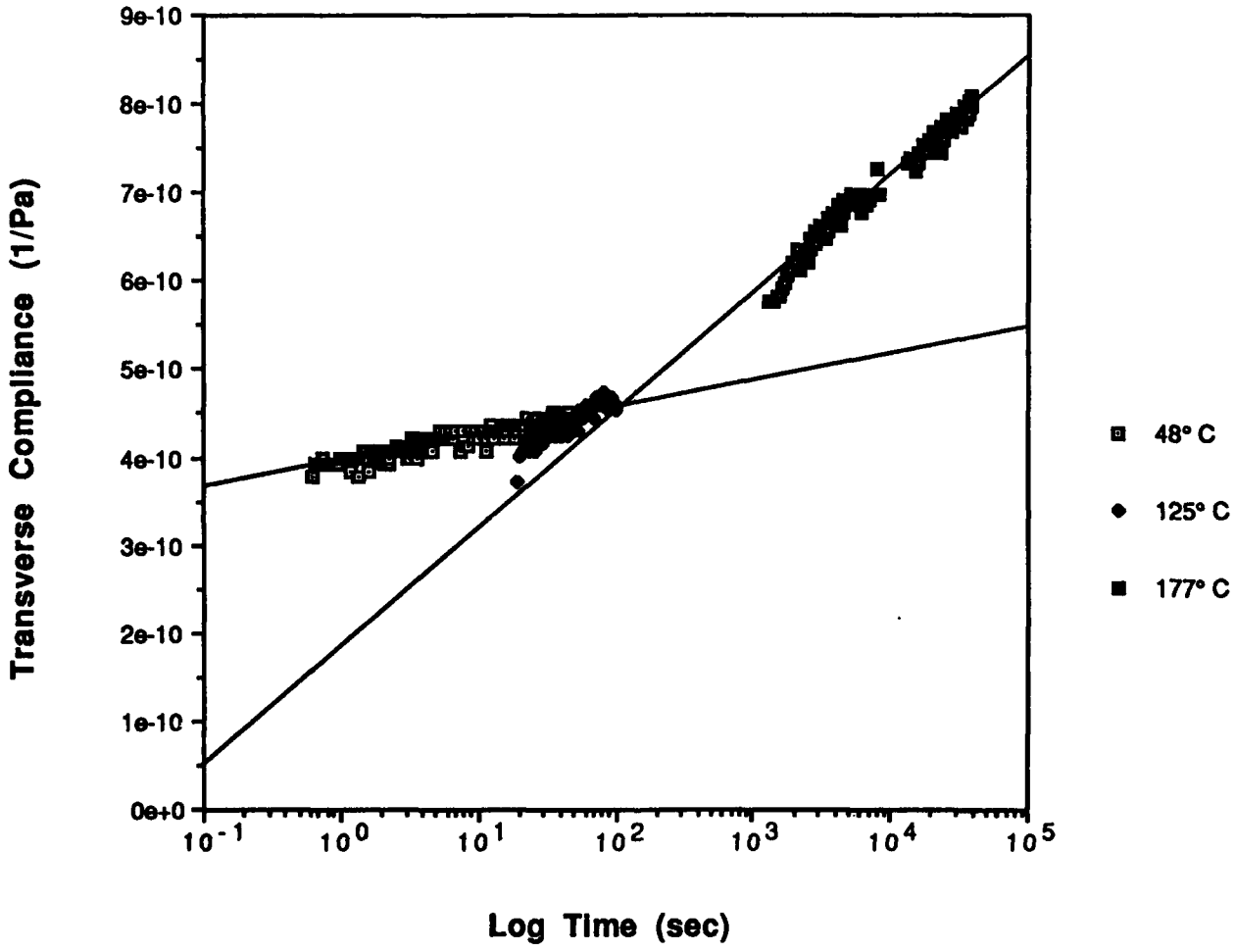

Figure 26. Time-Dependent Transverse Compliance Master Curve

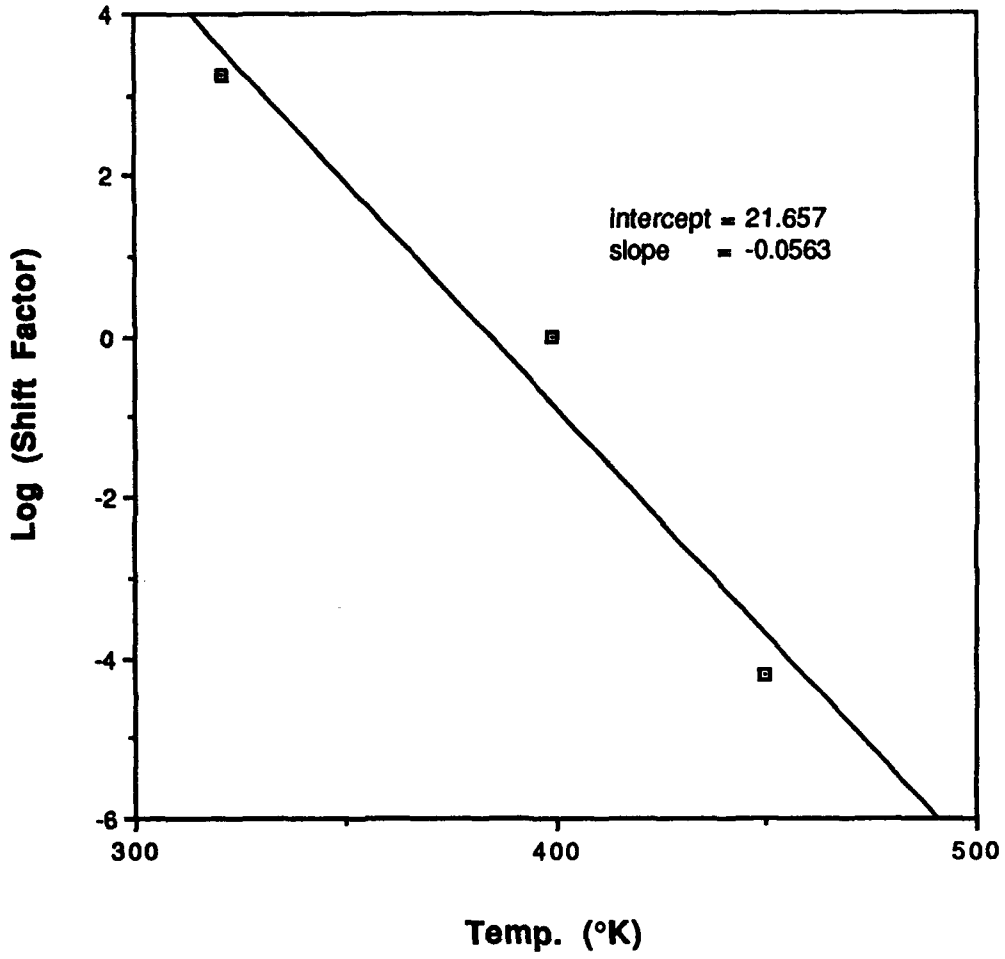

Figure 27. Shift Factor Parameter Fit IM6/3100 BMI

Table 4. Viscoelastic Model Input Data

Property	Value
A (°K)	17.7526
B	21.657
α_1	-0.27×10^{-6} /°C
α_2	29.592×10^{-6} /°C
S_{12}	-1.423×10^{-12} /Pa
S_1	5.4714×10^{-12} /Pa
n_{LR}	0.4648
n_{UP}	0.1118
D_{LR}	8.676×10^{-12} /Pa•sec$^{n_{LR}}$
D_{UP}	1.8953×10^{-10} /Pa•sec$^{n_{UP}}$
S_{22}^0 (LR)	1.142×10^{-10} /Pa
S_{22}^0 (UP)	4.428×10^{-11} /Pa

******* LR and UP signify lower and upper creep ranges

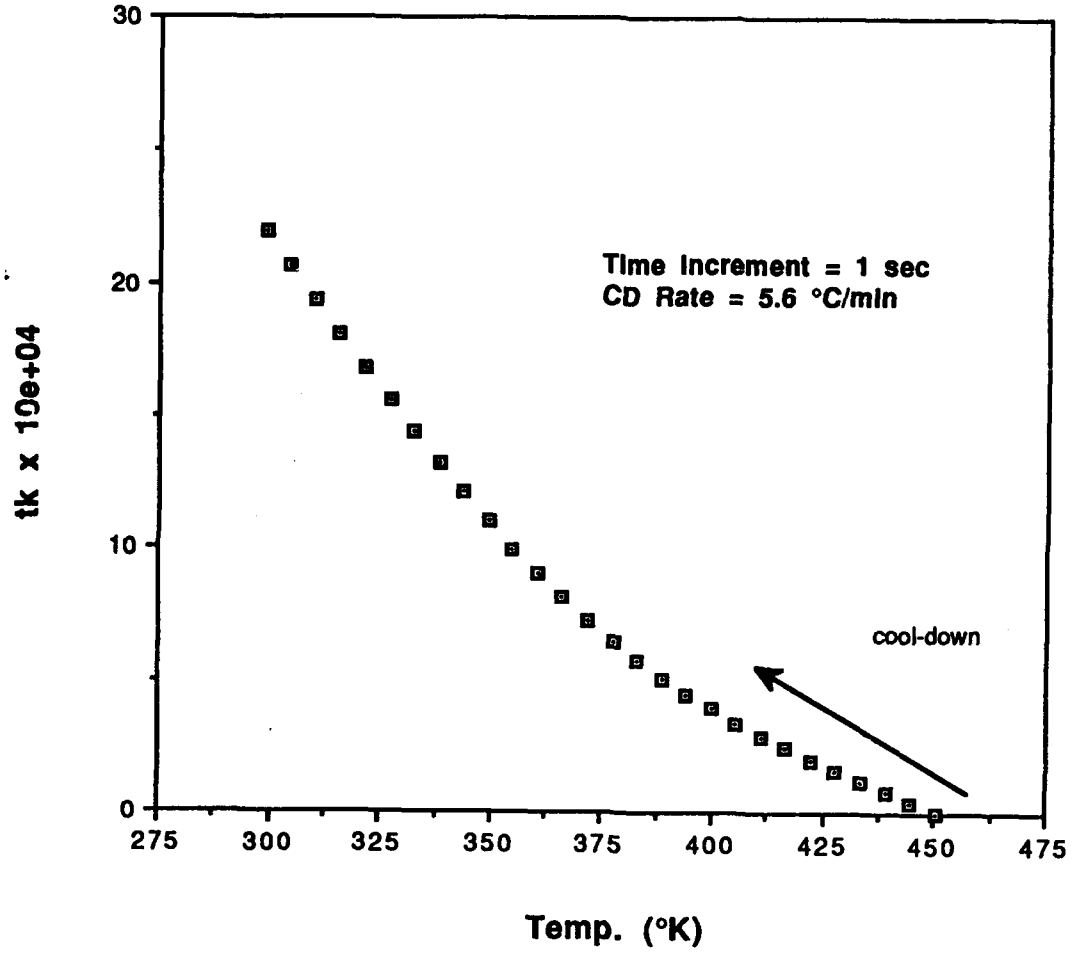

Figure 28. Dimensionless Curvature Development During Cool-Down (Viscoelastic Model)

4.8. Cure Cycle Optimization

One of the major objectives of the present research was to reduce residual stresses through optimization of the cure cycle parameters, i.e. temperature, pressure, and time. The data and analysis have shown that the dimensionless curvature can be predicted elastically by equation (7). Therefore, optimization cycles were selected to reduce the thermal strains induced during cure. Additionally, the effects of applied pressure and cool-down rate were investigated experimentally. Table 5 shows the cure cycles that were investigated.

4.8.1. Effect of Cure Temperature

Reducing the cure temperature will reduce the thermal strains experienced by the material. Therefore, as can be seen from equation (7), the induced curvature will be lowered. However, since most of the crosslinking occurs during the second dwell, the lower temperatures may have adverse effects on the mechanical properties and degree of cure.

For the first series of tests, cure cycles A, B, C1 and D were investigated. The results of this testing are shown in Figures 29(a) through (d). The dimensionless curvature of the non-postcured specimens is seen to decrease with decreasing cure temperature, as was expected. Between 340°F and 320°F a significant reduction in residual stress is obtained. However, this reduction is at the expense of transverse strength and modulus as can be seen in Figures 29(b) and (c). As was the case in the intermittently cured specimens in groups 7A and 8A, it is believed that specimens subjected to cure cycles C1 and D developed transverse cracks which reduced the dimensionless curvature beyond what can be predicted by elastic analysis.

Table 5. Processing Conditions for Cure Cycle Optimization Study

Cure Cycle	Cure Temp (°F)	Dwell Time (hrs)	Cool-Down Rate (°F/min)	Cool-Down Pressure (psi)	Cure Pressure (psi)
A	360	4	10	50	50
B	340	"	"	"	"
C1	320	"	"	"	"
C2	320	12	"	"	"
D	300	4	"	"	"
E	360	"	1	"	"
F	"	"	10	100	"
G	"	"	"	150	"

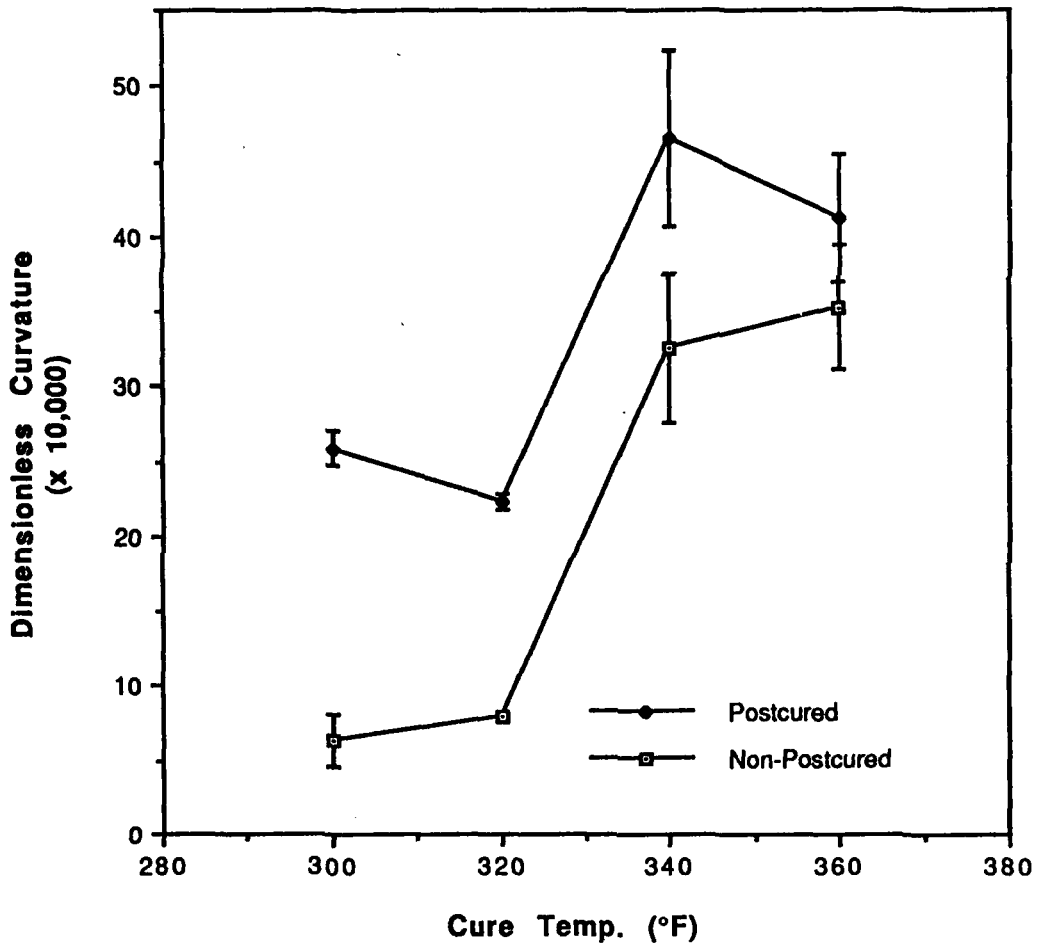

Figure 29(a). Cure Temperature Effect on Dimensionless Curvature (IM6/3100)

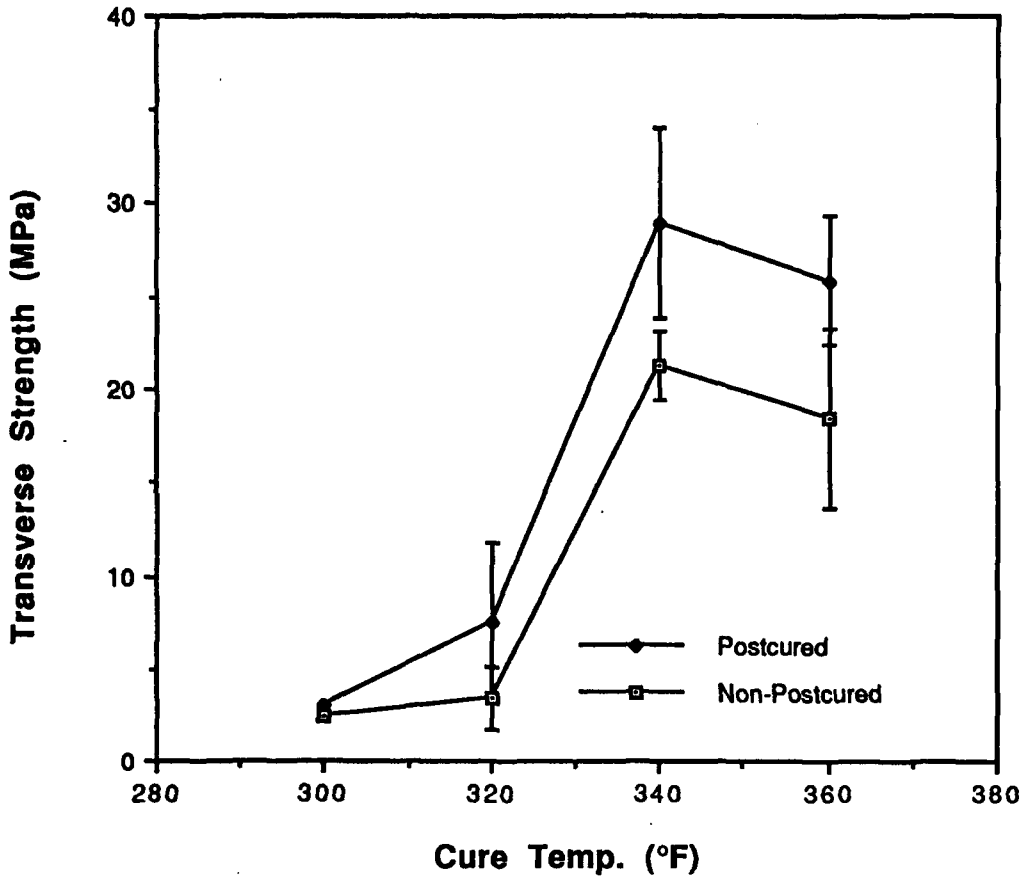

Figure 29(b). Cure Temperature Effect on Transverse Strength (IM6/3100)

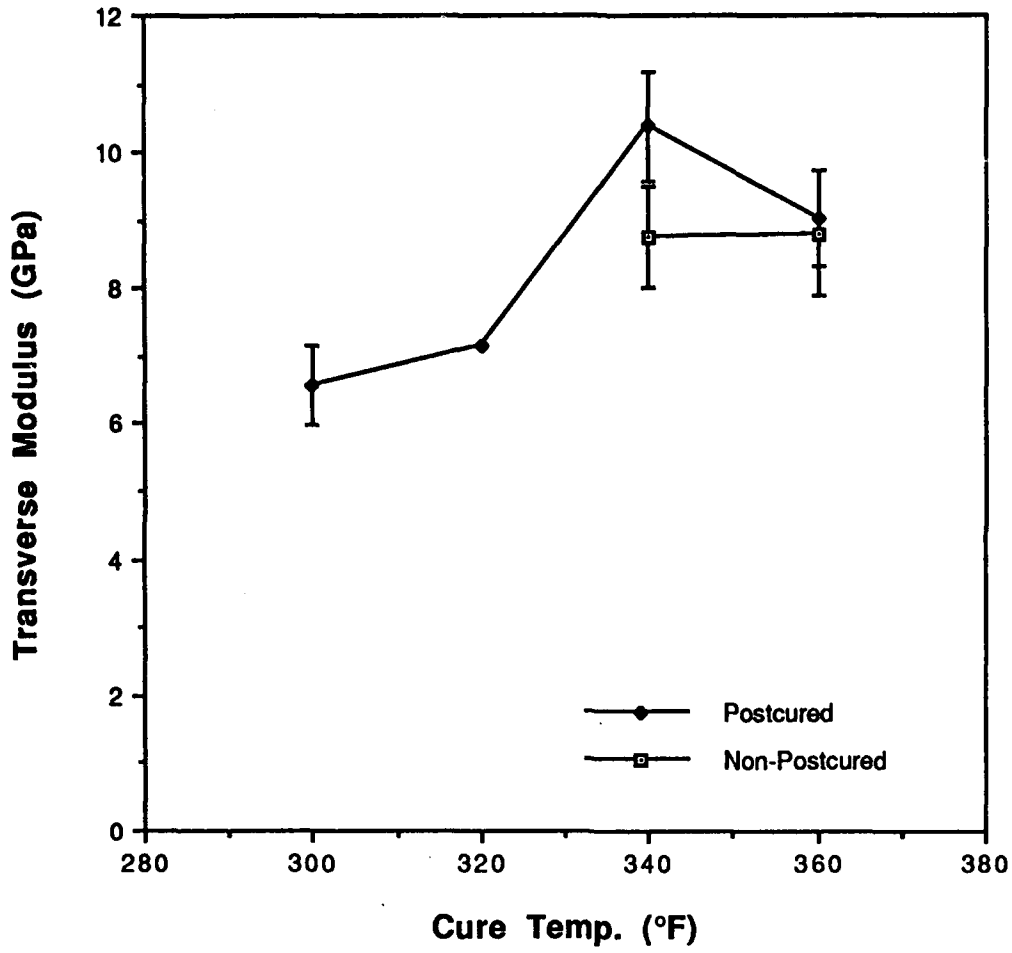

Figure 29(c). Cure Temperature Effect on Transverse Modulus (IM6/3100)

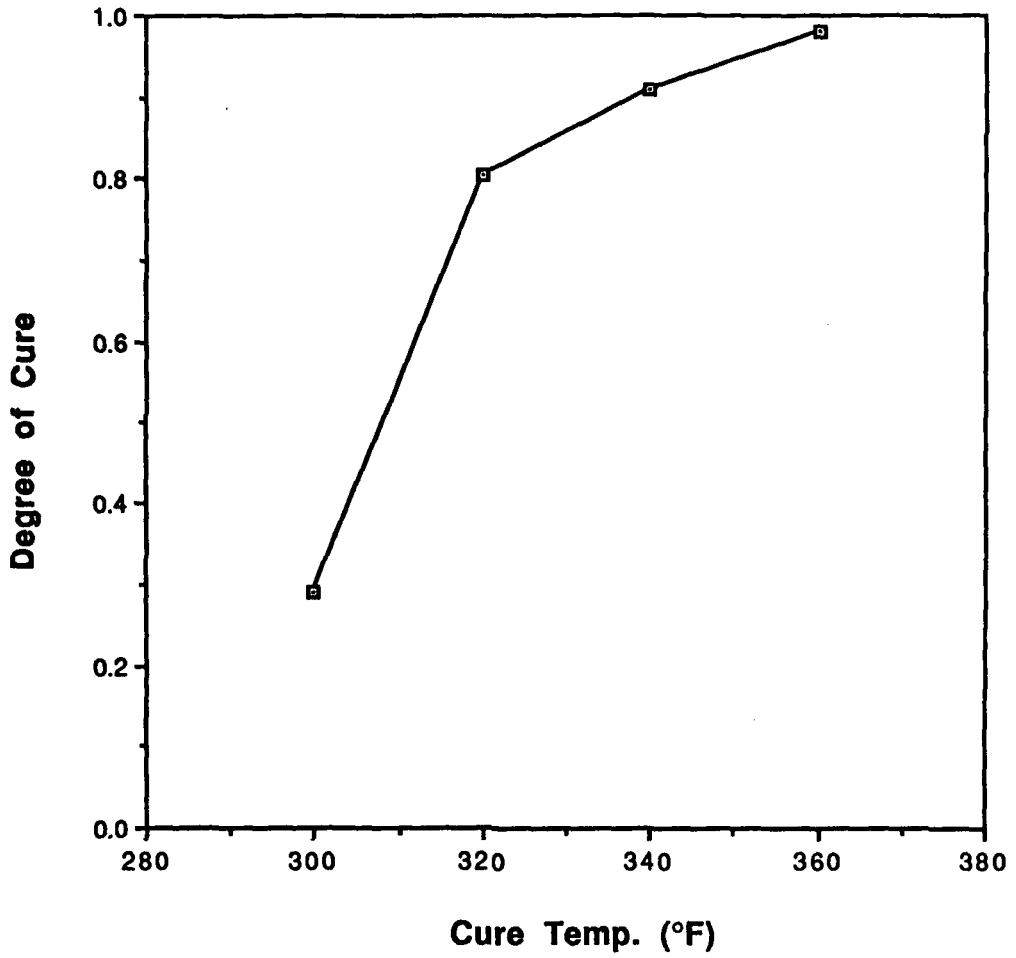

Figure 29(d). Cure Temperature Effect on Degree of Cure (IM6/3100)

The degree of cure of the specimens is seen to decrease as the cure temperature is lowered. DSC testing of postcured specimens showed that no appreciable residual exotherm could be measured. It is interesting to note that even though the postcured specimens are fully cured, their transverse strengths are still degraded for cure cycles C1 and D. The transverse cracks induced from primary cure will decrease the postcured transverse strength, but it is also plausible that different reactions are taking place at the various cure temperatures tested. At 360°F and 340°F, sufficient thermal energy is available in the primary cure cycle to obtain the desired strength in the cured laminate. However, at the lower cure temperatures in cycles C1 and D the fiber-matrix bonding may not be fully formed (see Figure 13) as well as the strength of crosslinks within the matrix material. After primary cure these characteristics are seen to remain.

Figure 29(a) shows that the 340°F cure specimens exhibits a higher curvature on the average after postcure than the standard 360 °F cured specimens. The increased transverse modulus of 340 °F specimens after postcure would account for the increase in curvature.

Reduced residual stresses seen in cycles C1 and D were promising; however, the reduction in mechanical properties was unacceptable. Therefore, cure cycle C2 was chosen to see if the degree of cure could be increased given a sufficient dwell time at 320 °F. DSC scans of C2 specimens gave a degree of cure between 0.94 and 0.96. Therefore, it is believed that the mechanical properties of these specimens will not be significantly degraded. The dimensionless curvature of these specimens were measured to be 28.60 with a standard deviation of 2.82. This represents a reduction in curvature of 14% from the MRC cycle. Using the fully cured mechanical properties and assuming the thermal strains are linearly related to the temperature difference, $\Delta T = T_{cure} - T_{RT}$, equation (7) predicts a curvature of 27.65. These results are very exciting since a significant reduction in dimensionless curvature was obtained while maintaining a reasonably full degree of cure.

These results show that by reducing the cure temperature and increasing the dwell time, the residual stresses can be reduced while maintaining the same mechanical properties. To analyze the optimum dwell time at various cure temperatures, the cure kinetics of the material must be developed.

4.8.2. Effect of Cool-Down Rate

The viscoelastic nature of polymer composite systems can be used during and after processing to relax residual stresses. Weitsman [7,10] has reported viscoelastic effects in his analysis of optimal cool-down profiles. Hedrick and Whiteside [19] reported viscoelastic relaxation in a 3501-6 epoxy system at a cooling rate of 1 °F/min. This viscoelastic relaxation is also manifested in relaxation of any chemical shrinkage strains that occur during the second dwell period of the MRC cycle. The viscoelastic relaxation of BMI was investigated by monitoring changes in the induced curvature when the cool-down rate was changed from 10 °F/min to 1 °F/min. All other processing parameters were held constant.

The transverse strength and modulus before and after postcure was not affected by the cool-down rates chosen as seen in Figures 30(b) and (c). DSC testing of the specimens showed no residual exotherm after postcure and no significant difference in degree of cure or T_g after the primary process cycle.

In Figure 30(a) a reduction in average curvature of 20% was seen for the non-postcured specimens. After postcure no significant change in curvature was achieved. Since the room temperature mechanical properties of both groups are the same and assuming that the thermal strains induced upon cool-down are the same, this reduction in residual stress could be attributed to viscoelastic stress relaxation. However, transverse cracking was not investigated for these specimens.

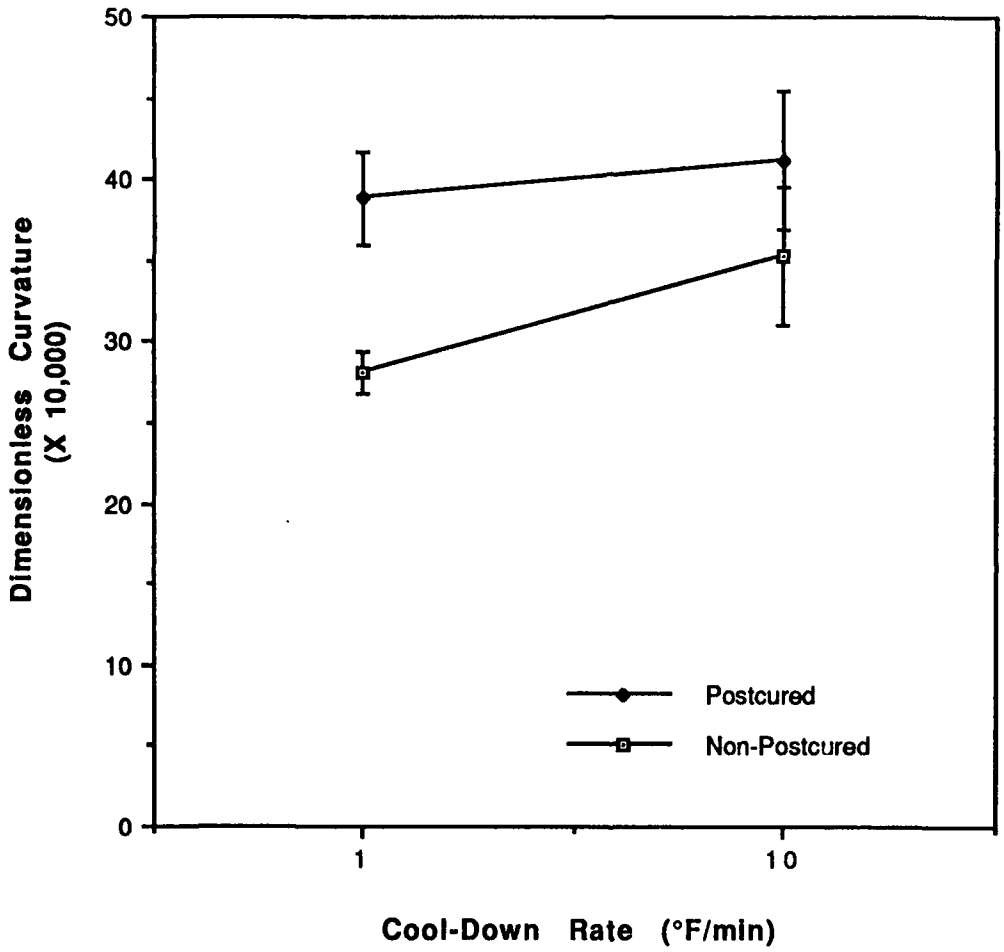

Figure 30(a). Cooling-Rate Effect on Dimensionless Curvature (IM6/3100)

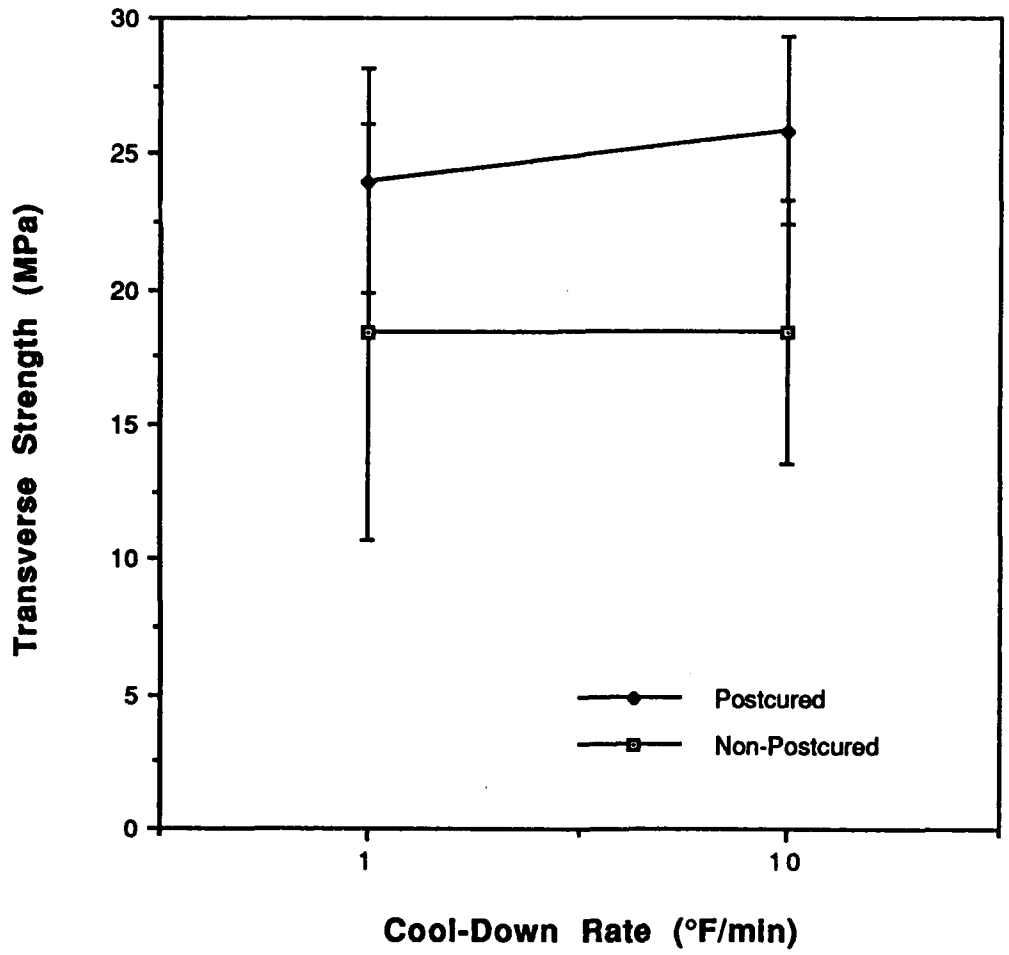

Figure 30(b). Cooling-Rate Effect on Transverse Strength (IM6/3100)

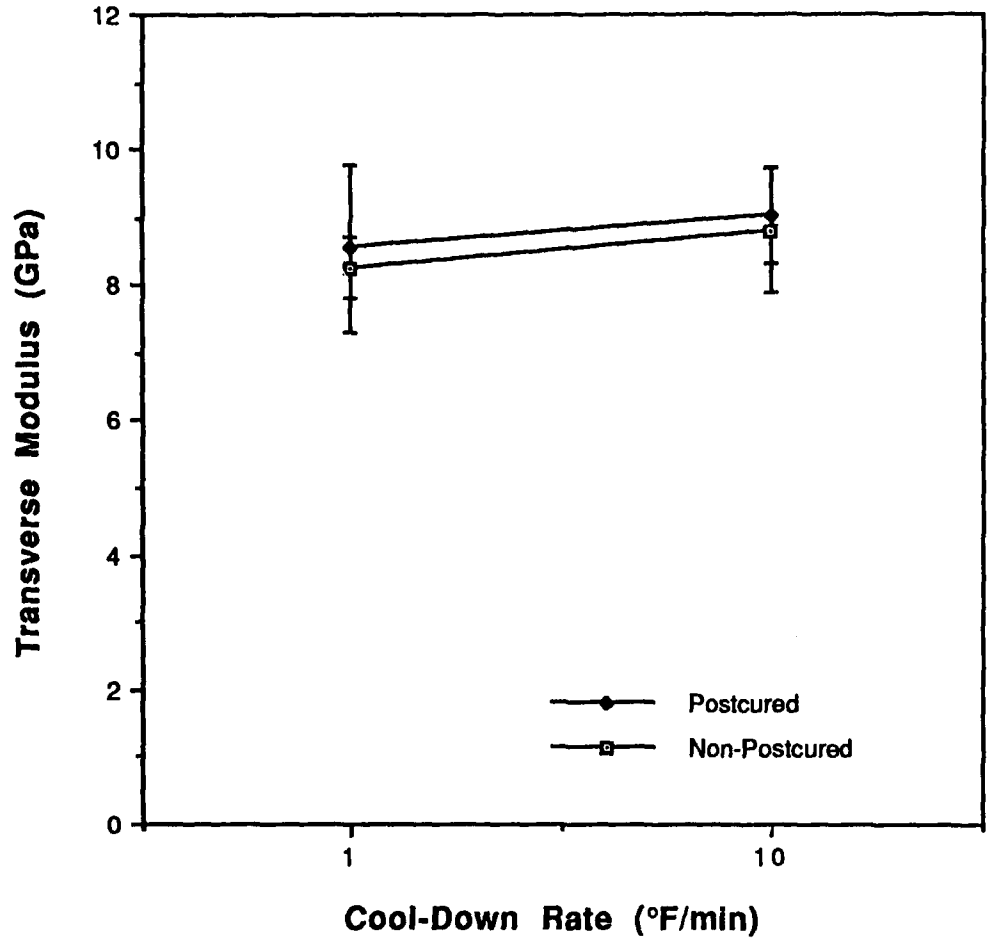

Figure 30(c). Cooling-Rate Effect on Transverse Modulus (IM6/3100)

4.8.3. Effect of Cool-Down Pressure

The applied pressure can affect the thermal expansion behavior of polymers as reported in [20]. Increasing in the applied pressure can decrease the thermal strains induced by a free volume argument. If an increased pressure were applied during the initial phases of the process cycle excessive resin flow could degrade the mechanical properties and structural integrity. Therefore, the effect of applied pressure was studied during the cool-down phase of the process cycle when the $c \approx 1$ and little resin flow is expected.

Figure 31(a) shows the changes in dimensionless curvature with three applied pressures: 50, 100, and 150 psi. For data both before and after postcure the residual stresses are reduced as applied pressure is increased. For the non-postcured specimens a reduction in dimensionless curvature of 7% was found for both 100 and 150 psi applied pressures. After postcure only data at 150 psi showed a significant reduction in curvature. The average curvatures at 150 psi and 50 psi give a reduction of about 16% after postcure.

The transverse strength of non-postcured specimens was significantly increased with increases in applied pressure. Some of this increase can be attributed to the reduction in residual stresses as evidenced by the reduction in dimensionless curvature. Other factors could include increased fiber/matrix adhesion and reduced void volume. After postcure the transverse strengths of the specimens at the three pressures are not significantly different.

DSC testing of the specimens showed no significant difference in degree of cure or T_g both before and after postcure. The same conclusions are drawn for the transverse modulus as seen in Figure 31(c). No statistical difference was seen before or after postcure for the applied pressures tested.

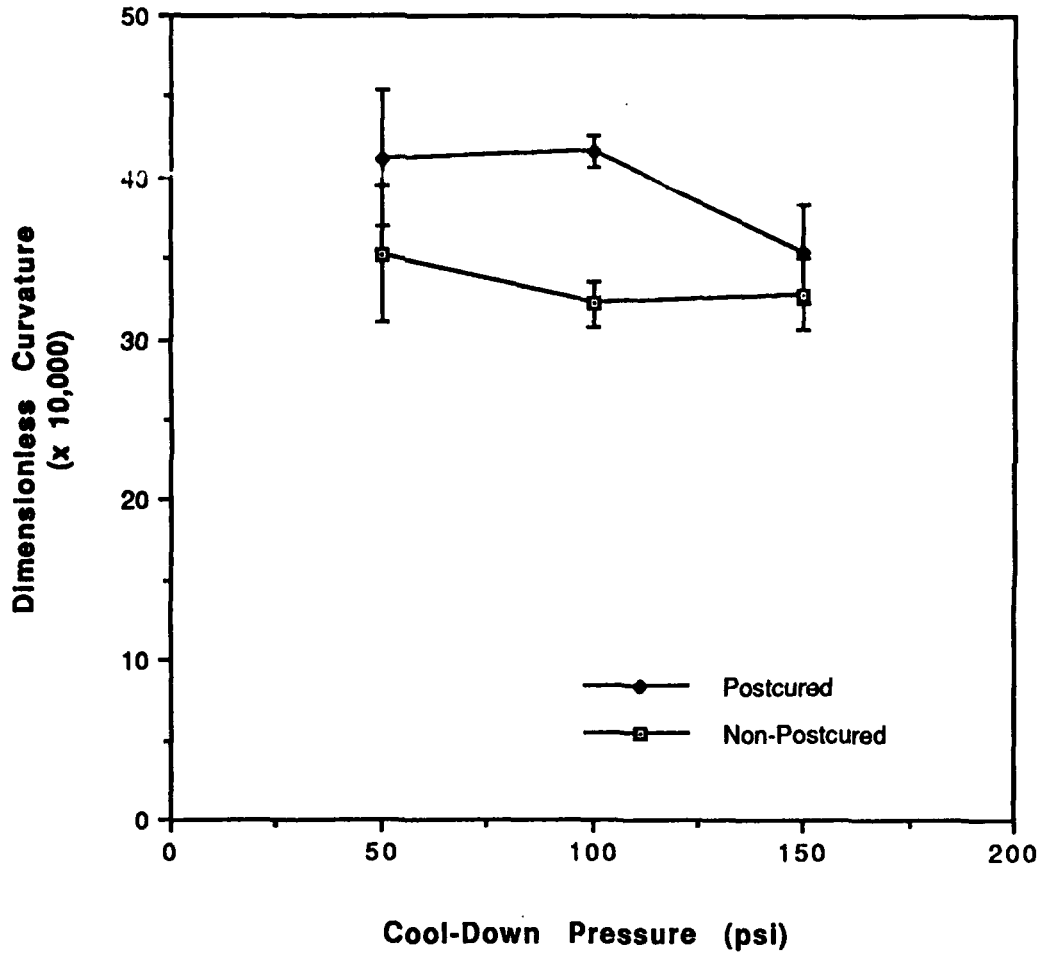

Figure 31(a). Cool-Down Pressure Effect on Dimensionless Curvature (IM6/3100)

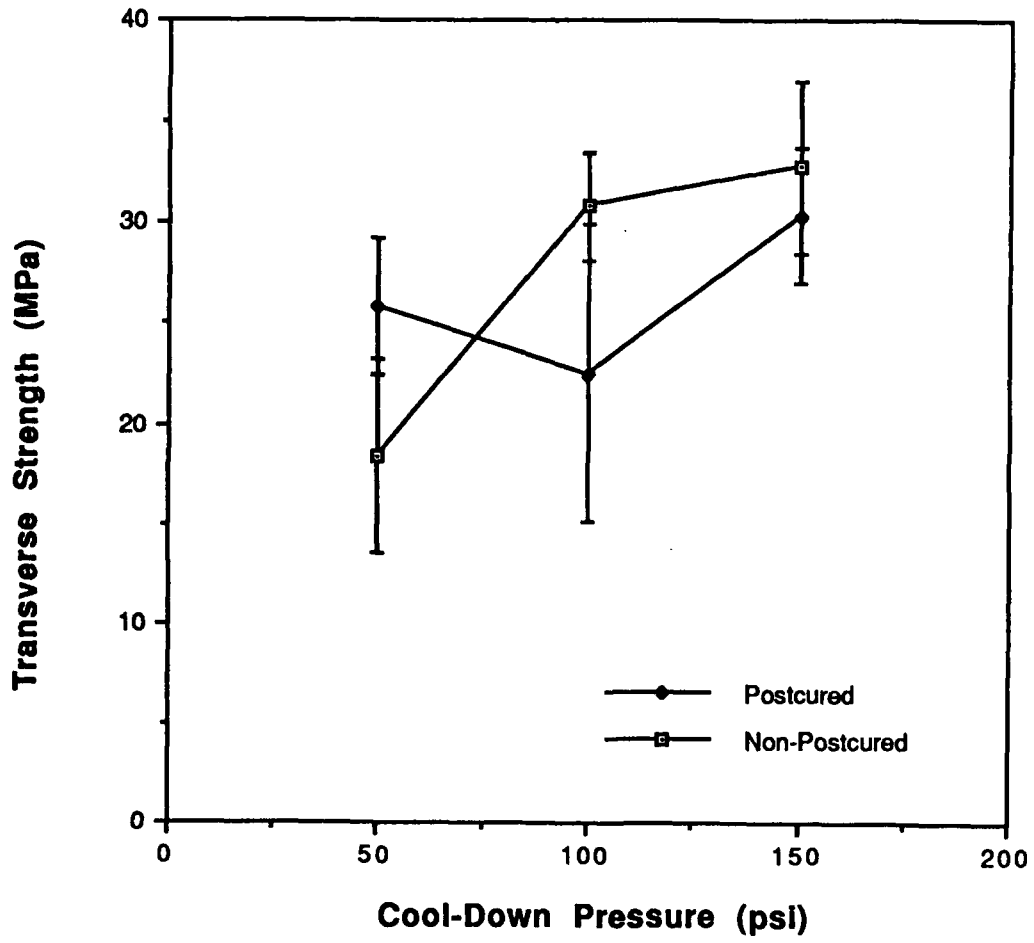

Figure 31(b). Cool-Down Pressure Effect on Transverse Strength (IM6/3100)

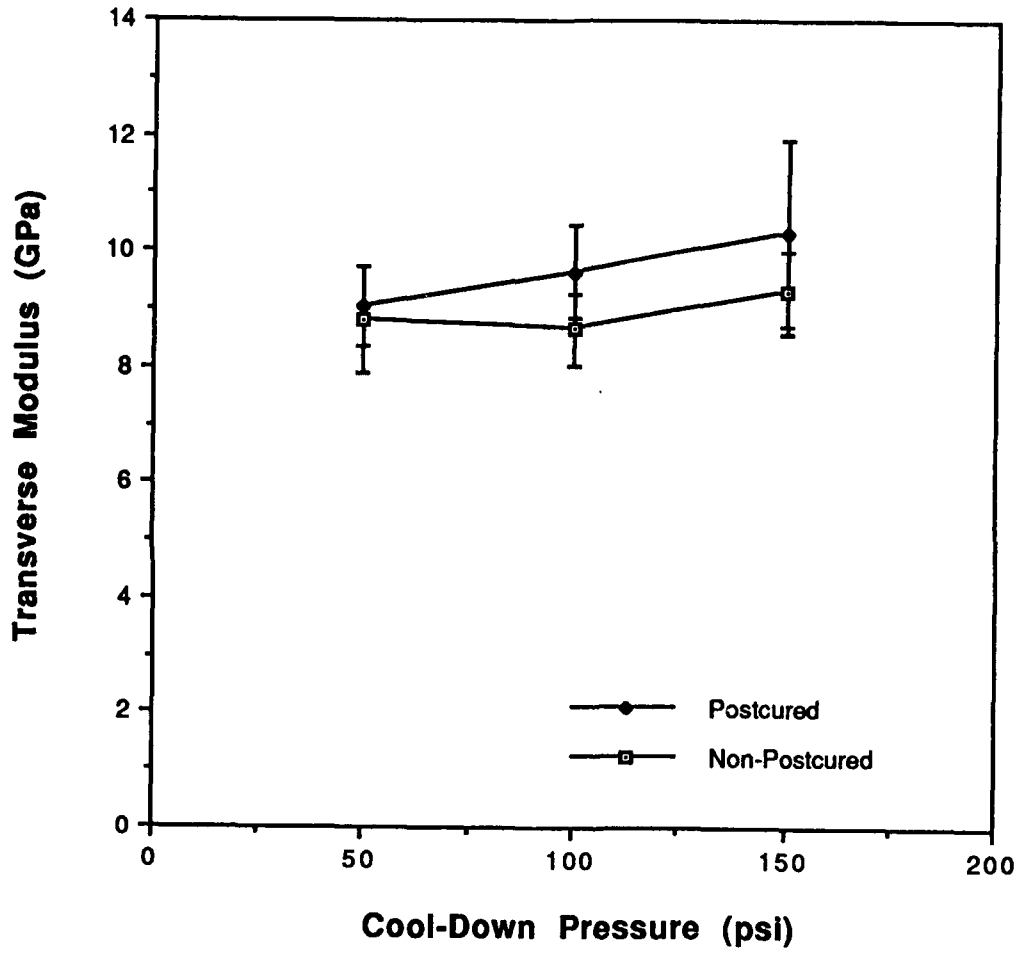

Figure 31(c). Cool-Down Pressure Effect on Transverse Modulus (IM6/3100)

5. Summary

The results of the analysis and testing during the grant period can be summarized in five significant conclusions.

1.) Equation (7) can be used to model the dimensionless curvature development during cure for BMI and, likewise, other thermosetting resin systems. Thus, the processing-induced residual stress development is quite elastic. If transverse cracking is developed, equation (7) will overestimate the curvature since transverse cracking relieves the residual stresses in the laminate.

2.) The transverse strength develops slower than the transverse modulus during cure. Therefore, transverse cracking can be developed if the degree of cure is not sufficient to allow transverse strength development. In the BMI system investigated, specimens with degrees of cure greater that 0.89 did not show signs of transverse cracking.

3.) Thermal strains are dominant in residual stress development in thermosetting resin systems. Chemical shrinkage strains and viscoelastic stress relaxation during cool-down were shown to be negligible for the processing conditions investigated.

4.) The residual stresses can be reduced by curing at lower temperatures. The mechanical properties and degree of cure are not sacrificed if dwell times are increased as well. Promising results were shown for BMI in which the residual stresses in the form of dimensionless curvature were reduced by 14% by processing at 320 F for 12 hours. The degree of cure in this case was 0.95 indicating a nearly complete reaction.

5.) An analytical optimization scheme should account for the cure kinetics of the resin. Knowledge of the cure kinetics will allow for optimum choice of dwell time and cure temperature to allow complete cure. Assuring complete cure is necessary to retain good mechanical properties after processing.

The recommended future work indicated by the present research should be the development of the cure kinetics of BMI. With this knowledge an analytical optimization scheme can be developed for reducing residual stresses while maintaining good mechanical properties.

The effect on residual stresses of cure cycles other than the MRC cycle or other closely related cycles should be investigated. The mechanical properties and transverse cracking behavior of processed specimens must then be investigated to understand the effect of these cycles on the overall performance of the processed composite.

6. Acknowledgement

The authors would like to acknowledge the support of the AFOSR with Lt. Col. George Haritos as grant monitor. Mr. John Masters of American Cyanamid is acknowledged for providing the material used in this study.

7. References

1. H. T. Hahn and N. J. Pagano, "Curing Stresses in Composite Laminates," *JCM*, Vol. 9, 1975, p. 91.

2. N. J. Pagano and H. T. Hahn, "Evaluation of Composite Curing Stress," *Composite Materials: Testing and Design* (4th. Conf.), ASTM STP 617, 1977, p. 317.

3. B. Harper, D. Peret, and Y. Weitsman, "Assessment of Chemical Cure-Shrinkage Stresses in Two Technical Resins," AIAA/ASME/ASCE/ AHS 24th Structures, Structural Dynamics and Materials Conf., Lake Tahoe, Nevada, May 2-4, 1983.

4. L. S. Penn, C. T. Chou, A. S. D. Wang and W. K. Binienda, "The Effect of Matrix Shrinkage on Damage Accumulation in Composites," submitted to *JCM* April 1989.

5. A. J. Armstrong, B. W. James, G. H. Wostenholm, B. Yates, J. Burgione, and J. Eastham, "Curing Characteristics of a Composite Matrix," *Journal of Materials Science*, Vol. 21, 1986, p. 4286.

6. B. D. Harper and Y. Weitsman, "Residual Thermal Stresses in an Unsymmetric Cross-ply Graphite/Epoxy Laminates," Proc. AIAA/ASME/ ASCE/AHS 22nd SSDM Conf., 1981, p. 325.

7. Y. Weitsman, "Residual Thermal Stresses due to Cool-Down of Epoxy Resin Composites," J. Appl. Mech., Vol 46, 1979, p. 563.

8. D. A. Douglas and Y. Weitsman, "Stresses Due to Environmental Conditioning of Cross-Ply Graphite/Epoxy Laminates," Proc. 3rd Int. Conf. on Composite Materials, Pergammon Press, 1980, p. 529.

9. D. L. Flaggs and F. W. Crossman, "Analysis of the Viscoelastic Response of Composite Laminates During Hygrothermal Exposure," *JCM*, Vol. 15, 1981, p. 286.

10. Y. Weitsman, "Optimal Cool-Down in Linear Viscoelasticity," *J. Appl. Mech.*, Vol. 47, 1980, p. 35.

11. M. W. Hyer, "Calculations of the Room-Temperature Shapes of Unsymmetric Laminates," *JCM*, Vol. 15, 1981, p. 296.

12. M. W. Hyer, "Some Observations on the Cured Shape of Thin Unsymmetric Laminates," *JCM*, Vol. 15, 1981, p. 175.

13. M. W. Hyer, "The Room-Temperature Shapes of Four-Layer Unsymmetric Cross-Ply Laminates," *JCM*, Vol.16, 1982, p. 318.

14. H. T. Hahn, "Warping of Unsymmetric Cross-Ply Graphite/Epoxy Laminates," *Composites Technology Review*, Vol. 3, 1981, p. 114.

15. A. Hamamoto and M. W. Hyer, "Temperature-Curvature Relationships for Unsymmetric Graphite-Epoxy Laminates," Tech. Report VPI-E-85-08, VPI & SU, March 1985.

16. H. T. Hahn, "Effects of Residual Stresses in Polymer Matrix Composites," *The Journal of Astronautical Sciences*, Vol. 32, 1984, p. 253.

17. Amijima, S. and Adachi, T., "Effect of Time on the Mechanical Behavior of Laminated Composites," Progress in Science and Engineering of Composites, ICCM-IV, Tokyo, 1982.

18. S.-Y. Lee and G. S. Springer, "Effect of Cure on the Mechanical Properties of Composites," *JCM*, Vol.22, Jan. 1988.

19. I. G. Hedrick and J. B. Whiteside, "Effects of Environment on Advanced Composites Structures," AIAA Conference on Aircraft Composites: The Emerging Methodology for Structural Assurance, San Diego, CA, March 24-25, 1977.

20. P. Zoller, "Specific Volume of Polysulfone as a Function of Temperature and Pressure," *Journal of Polymer Science: Polymer Physics Edition*, Vol.16, 1978, p. 1261.